


Optical trapping gets structure: Structured light for advanced optical manipulation ^F

Cite as: Appl. Phys. Rev. 7, 041308 (2020); <https://doi.org/10.1063/5.0013276>

Submitted: 09 May 2020 . Accepted: 04 November 2020 . Published Online: 25 November 2020

 E. Otte, and  C. Denz

COLLECTIONS

 This paper was selected as Featured



View Online



Export Citation



CrossMark



Overachiever.

APR's 17.054 Journal Impact Factor makes your decision of where to publish much easier.

SUBMIT NOW!



Applied Physics Reviews

17.054
14.588
12.577

Optical trapping gets structure: Structured light for advanced optical manipulation

Cite as: Appl. Phys. Rev. **7**, 041308 (2020); doi: [10.1063/5.0013276](https://doi.org/10.1063/5.0013276)

Submitted: 9 May 2020 · Accepted: 4 November 2020 ·

Published Online: 25 November 2020



View Online



Export Citation



CrossMark

E. Otte^{a)}  and C. Denz 

AFFILIATIONS

Institute of Applied Physics, University of Muenster, Corrensstr. 2/4, 48149 Münster, Germany

^{a)} Author to whom correspondence should be addressed: eileen.otte@uni-muenster.de

ABSTRACT

The pace of innovations in the field of optical trapping has ramped up in the past couple of years. The implementation of structured light, leading to groundbreaking inventions such as high-resolution microscopy or optical communication, has unveiled the unexplored potential for optical trapping. Advancing from a single Gaussian light field as trapping potential, optical tweezers have gotten more and more structure; innovative trapping landscapes have been developed, starting from multiple traps realized by holographic optical tweezers, via complex scalar light fields sculpted in amplitude and phase, up to polarization-structured and highly confined vectorial beams. In this article, we provide a timely overview on recent advances in advanced optical trapping and discuss future perspectives given by the combination of optical manipulation with the emerging field of structured light.

Published under license by AIP Publishing. <https://doi.org/10.1063/5.0013276>

TABLE OF CONTENTS

I. INTRODUCTION	1
II. FROM THE TAILS OF COMETS TO HOLOGRAPHIC OPTICAL TWEEZERS.....	3
A. Conventional optical tweezers	3
B. Holographic optical tweezers.....	4
III. TAILORED SCALAR LIGHT AS ADVANCED TRAPPING POTENTIALS.....	4
A. From standard 2D to elegant 3D structured Gaussian potentials.....	5
B. 3D particle control by tailored propagation of light.....	6
C. Intensity singularities in 3D caustic light fields...	7
IV. ENERGY FLOW DENSITY AND OPTICAL ANGULAR MOMENTA	7
A. Fundamental properties.....	7
B. Customized phase flow.....	9
C. OAM beams for optical metrology	9
V. VECTORIAL LIGHT AS A PIONEERING TOOL FOR OPTICAL MANIPULATION	10
A. Superposition principle and customized SFD structures	10
B. From single-beam approaches to fully-structured light.....	12
C. Shaping polarization in 3D space.....	13

VI. FOCAL FULLY-STRUCTURED TRAPPING LANDSCAPES	13
A. Basic vector fields for optical trapping	14
B. Focal field customization by polarization modulation.....	14
C. 3D polarization topology, its analysis and future potential	16
VII. CONCLUSION.....	17

I. INTRODUCTION

In 2018, Arthur Ashkin was awarded the Nobel Prize for his groundbreaking development of optical trapping, which he introduced in 1970.¹ Nowadays, this technique is well established and used in a vast number of advanced applications ranging from sensitive rheological metrology^{2–4} to the study of DNA by, for instance, stretching single chromatin fibers⁵ or the formation of 2D and 3D reconfigurable particle assemblies,^{6,7} shaping, e.g., hybrid soft matter,⁸ or functional, responsive, and even intelligent nano-materials.⁹ In the conventional, yet powerful trapping configuration [Fig. 1(a)], a single Gaussian light field is applied for particle manipulation by a combination of optical gradient and scattering forces.¹ By adding more than a single trap by acousto-optical, multiplexing, or holographic techniques, light started in a simple way to get structured. However, from these first approaches to fully-structured light, simultaneously spatially varying

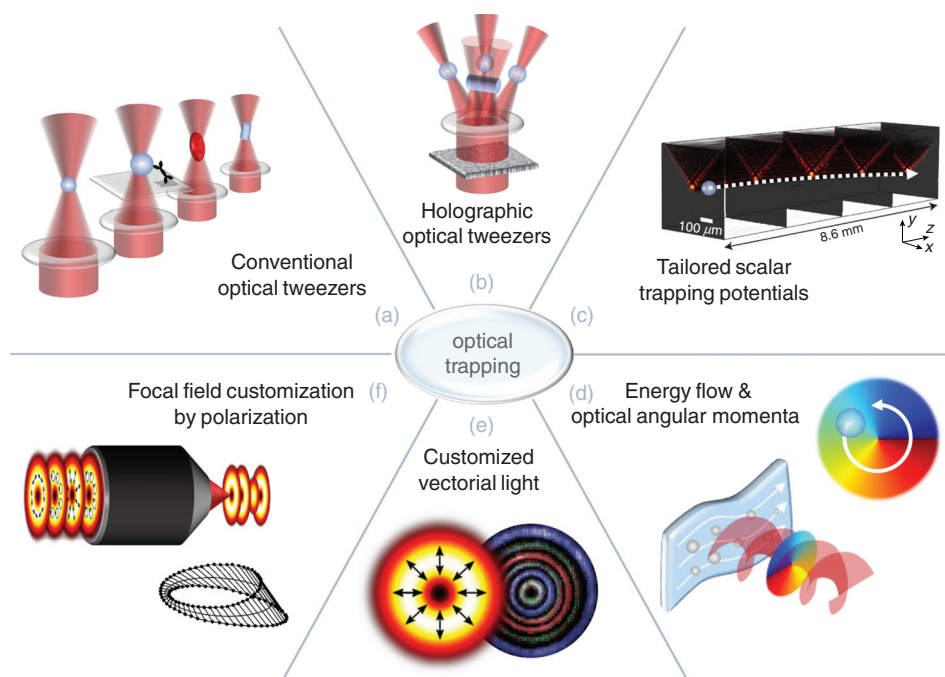


FIG. 1. In the conventional trapping configuration, a single Gaussian light field is applied for particle manipulation by a combination of optical gradient and scattering forces (a); schematic of holographic optical tweezers enabling dynamic multi-particle manipulation (b); a scalar light field can be tailored to include a transverse as well as longitudinal on-demand variation in intensity and phase paving the way for two- (2D) or disruptive three-dimensional (3D) trapping potentials (c); scalar structured light represents another useful tool in optical manipulation, as it allows scalar fields to carry orbital angular momentum (d); and implementation of polarization modulation and tight focusing as powerful customization tools for next-generation optical trapping [(e) and (f)].

in its amplitude, phase, as well as polarization, it is a long and successful way of numerous inventions.

Different approaches of structured light have already proven their impact in different fields of applied physics, in microscopy as well as in classical or quantum information technologies.¹⁰ For instance, in light sheet microscopy,^{11,12} the illuminating light field is shaped by a cylindrical lens to reduce the background noise of fluorescence, while in stimulated emission depletion (STED) microscopy,¹³ a ring-shaped intensity structure allows for spatial resolution beyond the diffraction limit. Furthermore, for advanced data communication as well as higher-dimensional quantum key distribution (QKD), simple transverse light structures are used to encode additional information in the spatial degrees of freedom of light. To enlarge the transmission bandwidth in communication or increase the dimension in QKD and, thereby, information capacity per photon, spatial modes of light such as Laguerre–Gaussian (LG), Hermite–Gaussian (HG), or cylindrical vector beams (CVBs) are implemented (see, e.g., Refs. 14–20).

Within the field of optical trapping, already basic structures of light enabled an important milestone: in 1998, Dufresne and Gier introduced holographic optical multiple-particle trapping by transferring a single light field into multiple trapping beams via micro-fabricated diffractive optical elements.²¹ Advancing from this principle, in 2000, Liesener *et al.* developed holographic optical tweezers [HOT; Fig. 1(b)].^{22,23} By digital lenses-and-grating holograms, they demonstrated simultaneous, dynamic manipulation of various micro-objects. This advancement has been enabled by the implementation of a spatial light modulator (SLM), allowing for phase and amplitude modification depending on the displayed hologram.^{24,25} Nowadays, advanced HOT represents an established tool for precise light-assisted assembly of micro- or nano-objects (see, e.g., Refs. 6, 7, 9, 26–28), opening new avenues for the controlled fabrication of functional nano- and meta-materials. HOT has been applied for automated

trapping, assembling and sorting colloidal particles,⁷ controlling light-driven micro-tools fabricated by two-photon polymerization,^{28,29} to create bio-hybrid micro-machines,³⁰ or for the light-driven assembly of functionalized organic nano-containers.⁸

However, trapping multiple objects at a time is not necessarily linked to HOT. A more advanced approach is to modulate the amplitude and phase of light in such a way that a single, but complexly structured beam is created, where every intensity spot is acting as a single optical trap. This scalar light field can be tailored to include a transverse as well as longitudinal on-demand variation in intensity and phase, paving the way for two- (2D) or disruptive three-dimensional (3D) trapping potentials^{31–38} [Fig. 1(c)]. A simple example is a higher-order Gaussian beam, e.g., a Hermite–Gaussian mode, in which each transverse intensity lobe can act as a separate trap. More advanced examples of complex trapping landscapes created by a single light field are arbitrarily shaped fields^{38–40} or optical tractor beams,^{36,39} as well as accelerated, caustic light fields³⁷ with 3D varying intensity structures. Such fields allow trapping and attracting multiple objects simultaneously or guiding particles on curved trajectories, respectively. Beyond, the spatially varying phase of scalar structured light represents another useful tool in optical manipulation, as it allows scalar fields to carry orbital angular momentum (OAM)⁴¹ [Fig. 1(d)]. This property laid the foundation for the nowadays well-known ability to orbit particles in optical tweezers around a central area,^{42–45} which enabled, e.g., the realization of an optical tractor beam (optical solenoid beam) based on a combination of OAM transfer and arbitrarily shaped 3D intensity landscape.³⁹ In addition, light-matter-interaction of these OAM-beams has unlocked innovative approaches for metrology: it allows analyzing, e.g., the vorticity in fluids⁴⁶ or the activity in chiral molecules.⁴⁷

In addition to amplitude and phase, the polarization of light also plays a major role in optical trapping today. The polarization

handedness is related to the spin angular momentum (SAM) of light, which is transferable to trapped objects. Already before the implementation of structured light, SAM was proven to be a means to spin birefringent objects in conventional optical tweezers.⁴⁸ Crucially, polarization has today become another degree of freedom of light, which can be shaped spatially within a trapping beam, opening new perspectives for optical tweezers. On the one hand, spatial polarization modulation, i.e., vectorial light [Fig. 1(e)], is of specific interest for trapping and arranging polarization-sensitive objects. On the other hand, polarization modification allows spatially customizing SAM and the spin part of the transverse energy (Poynting vector) flow,^{45,49,50} which then can be in turn transferred to trapped objects. Together with the ongoing development of light shaping techniques, this field of research is evolving quickly, contributing significantly to the advancement of optical trapping.

Combining amplitude, phase, and polarization modulation allows for the joining of the above-mentioned trapping properties of scalar as well as vectorial light. For instance, this approach facilitates joint orbital and spin angular momentum modification^{51–53} in 2D or 3D structured light landscapes. This ability will have a tremendous impact on future optical trapping applications, enabling on-demand 3D manipulation of trapped objects. By this combination of on-demand spatial amplitude, phase, and polarization variation, the so-called fully-structured fields^{52,54,55} become available—i.e., optical trapping gets full structure.

Finally, to bring the full structure to the nanoscale and, thereby, drive next-generation optical trapping in confined environments, tightly focusing vectorial light is a cutting-edge approach [Fig. 1(f)]. Tight focusing enables the formation of significant longitudinal polarization components,^{56,57} representing an additional degree of freedom in fully-structured non-paraxial light, which can be customized in any desired way. In that spirit, fully-structuring light has allowed for a recently presented HOT upgrade: the vector holographic optical trap,⁵⁸ implementing multiple tightly focused vectorial fields. In general, tight focusing allows for novel trapping landscapes, adjustable trapping forces, and energy flow, as well as complex topological structures as polarization Möbius strips (see, e.g., Refs. 59–66). Among these, topological structures of 3D polarization states will revolutionize the trapping of polarization-sensitive micro- or nano-objects, allowing for the formation of functional micro- and nano-network structures and intelligent matter with, for instance, object orientation following the tailored, 3D twisted polarization topology of Möbius strips.

In the following, we will elucidate this path from elementary structured light-based trapping approaches to the implementation of fully-structured non-paraxial light. First, we will introduce the principles of optical tweezers and outline the evolution from studying the orientation of tails of comets to HOT, presenting exemplary applications (Sec. II). Beyond realizing multiple dynamic trapping beams by HOT, in Sec. III we highlight customized 2D and 3D trapping potentials by combining amplitude and phase modulation. Subsequently, the role of energy flow and optical angular momentum is elucidated, in particular highlighting the role of transverse phase structuring, applied in optical trapping and metrology (Sec. IV). Furthermore, we highlight a timely approach for SAM as well as combined OAM and SAM modulation. Therefore, next-generation optical trapping based on polarization modulation and fully-structuring light is presented in Sec. V. This modulation of light also enables the customization of focal

trapping landscapes as presented in the last Sec. VI, including recent findings on their exotic properties, opening new perspectives for advanced optical manipulation.

II. FROM THE TAILS OF COMETS TO HOLOGRAPHIC OPTICAL TWEEZERS

A. Conventional optical tweezers

When light is refracted, absorbed, or reflected by a small particle, both light and particle generally experience a change in momentum by the fundamental action-reaction principle of Newton. Already in 1619, Kepler suggested this transfer of momentum or, more precisely, the corresponding optical force to be the cause of tails of comets pointing away from the sun.⁶⁷ Confirming this suggestion by the electromagnetic theory,⁶⁸ Maxwell associated not only energy but also linear momentum with light waves, which was, subsequently, proven qualitatively^{67,69} as well as quantitatively⁷⁰ by Lebedev and Nichols and Hull. Finally, Ashkin put radiation force into practice by developing the concept of counter-propagating optical trapping.¹ Today, this groundbreaking work is considered as the birth of optical tweezers.

In order to realize a stable 3D confinement of particles, the radiation pressure of two opposed laser beams is applied [see Fig. 2(a)]. Therefore, Ashkin did not only observe the scattering force of light, being proportional to the intensity of light ($\vec{F}_{\text{scat}} \propto I$), but also the gradient force, pulling transparent objects (of higher refractive index than the surrounding medium) toward areas of highest intensity ($\vec{F}_{\text{grad}} \propto \vec{\nabla} I$).⁷¹ Later, the knowledge about these forces was transferred to what is today known as (conventional) optical tweezers: by tightly focusing a single laser beam by means of a high numerical aperture (NA) lens, strong gradient forces are created, counteracting the scattering forces in the propagation direction [see Fig. 2(b)]. This

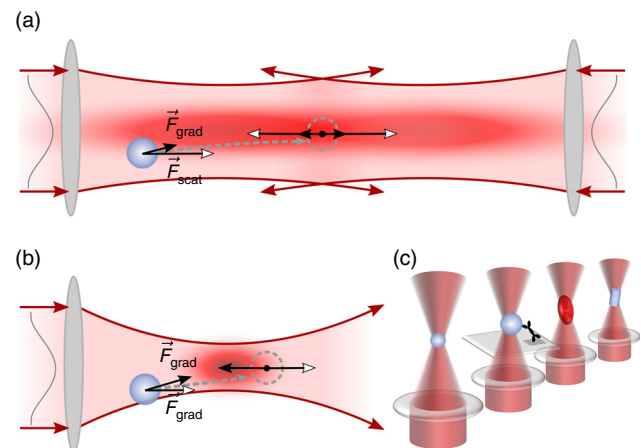


FIG. 2. The principle of optical trapping. To realize a stable 3D confinement of particles, the radiation pressure of two opposed laser beams can be applied. In (a), the respective counterpropagating optical trapping scheme is illustrated. (b) In conventional optical tweezers, by tightly focusing a single laser beam by means of a high numerical aperture lens, strong gradient forces (\vec{F}_{grad}) are created, counteracting the scattering forces (\vec{F}_{scat}) in the propagation direction (dashed circle: equilibrium position). (c) Examples of trapped objects in an optical tweezers (left to right): transparent bead, transparent bead for motor protein analysis, red blood cell, and cylindrical particle.

elegant method leads to a stable optical trapping of dielectric particles of various different properties in three dimensions and paved the way for a broad range of applications [see Fig. 2(c)]. For his invention of optical tweezers and its application to biological systems, Ashkin was awarded the Nobel Prize in Physics 2018.

With respect to applications, conventional optical tweezers enables handling single cells, organelles, or macromolecules without physical contact, i.e., non-invasively, making it an unrivaled tool for addressing biological questions.^{72–74} Furthermore, optical tweezers allows exerting defined and measuring extremely small forces in the range of pico-Newton with high precision,^{75–79} enabling the investigation of inter- and intra-cellular processes being responsible for reproduction, signaling, or respiration. Optical tweezers for biological and medical applications has been reviewed extensively, even very recently, so that we refer the interested reader to Refs. 80–83. In addition, many other fields of research as colloidal science,⁸⁴ particle separation and sorting,^{85–87} or microfluidics,^{85,88} among others, have and still do benefit from conventional optical tweezers. For instance, in nanophysics, the ability to organize matter non-invasively facilitated pioneering studies in the field of classical statistical mechanics as the first direct measurement of macromolecular interactions in solution.^{89,90}

In some of the named implementations, the conventional optical trap is dynamically moved by mechanically adapting the beam incident on the focusing high-NA lens or microscope objective (MO). By changing the beam's input angle on the MO, the trap's transverse position can be varied, while changes of the divergence of the input beam affect the longitudinal trap position. Additionally, the implementation of two or more trapping beams can also be realized mechanically by beam splitting. As introduced by Dufresne and Gier,²¹ holographically, multiple trapping beams can be shaped by diffractive optical elements. The increasing demand on creating more than two, possibly multiple dynamic traps led to the pioneering advancement to holographic optical tweezers based on a SLM, first presented by Liesener *et al.* in 2000.^{22,23}

B. Holographic optical tweezers

Holographic optical tweezers (HOT) represents a key advancement in the history of optical trapping, as it allows for the digital transformation of a single beam into multiple trapping beams [Fig. 1(b)], being dynamically and independently adjustable in all three spatial degrees of freedom. This transformation is typically performed by computer-generated, thus, digital holograms (CGHs). While at the dawn of the 21st century, these computer-generated holograms were often realized by static polymeric or silver halogenide holograms; nowadays, SLMs have become versatile standard tools for this function. As outlined in Ref. 22, a complex superposition of multiple phase gratings and holographic lenses is encoded on the SLM to emulate the number of traps in three dimensions. To allow for a dynamic adjustment of traps, computer-addressable phase-only SLMs are typically employed,⁹¹ positioned in the conjugated (Fourier) plane of the trapping plane. Since the gratings-and-lenses approach requires low computational expense and the SLM allows for a sufficiently fast variation of displayed CGHs, traps can be dynamically moved in real-time. If high-speed trap movement in the kHz regime is desired, digital mirror devices (DMDs) can be implemented, replacing SLMs. Note that, despite its advantages, HOT also suffers from the so-called ghost traps or inhomogeneities of individual traps. To overcome these drawbacks, different approaches have been suggested.^{92–96} For instance, iterative Fourier transformation

algorithms^{97,98} can be used for optimization considering, e.g., the pattern of the trapping beam, possible pixelation and discretization of the phase levels, suppression of ghost traps, or other inhomogeneity. Note that the trapping of complex objects as nanocontainers or arbitrary shaped particles is even today a challenging topic and thus subject to ongoing research. For example, a recent study by O'Brien and Grier²⁶ has shown that colloidal spheres trapped by HOT tend to move farther along the axial direction than the trap potential suggests, highlighting the demand for further advancements in HOT by, e.g., real-time feedback systems.

However, for already 20 years HOT has enabled numerous applications. It was implemented for the experimental investigation of infection scenarios at the single cell level,²⁷ for the operation of and sensing in lab-on-a-chip devices,⁹⁹ for 3D assembly of colloidal particles in a micro-channel,¹⁰⁰ or for arranging and orienting non-spherical objects.⁴⁵ Trapping non-spherical objects by HOT even facilitated the realization of bio-hybrid micro-robots by bringing together nano-containers as carriers and motile flagellated bacteria as the propelling living organism.³⁰ Nano-containers were also used to shape hybrid soft matter.⁸ For this purpose, Barroso *et al.* assembled surface-functionalized nanoporous zeolite-L crystals by HOT to construct arbitrary 3D nanoarchitectures, as exemplified by the schematic representation in Fig. 3(a). As the zeolites carry a functionalized polymer shell, the controlled, instant, and highly efficient particle–particle and particle–surface adhesion is enabled. Crucially, shaped architectures remain permanently stable after release from the HOT system, as it is proven by guiding [Fig. 3(b)] an unbound crystal (red circle) freely underneath the constructed arch from left to right.

Recently, HOT was also applied to operate micro-rotors to perform reconfigurable hydrodynamic arrangements and, thereby, indirect optical trapping,²⁸ as illustrated in Figs. 3(c)–3(g). The laser-printed micro-rotors are trapped and rotated by HOT. By a feedback control loop combined with a SLM, the desired flow-field is continuously designed for a specific tracked target and realized by encoding the respective hologram on the SLM, driving the rotor motion. This approach enables guiding and embedding absorbing objects by the flow field, as schematically shown in Fig. 3(c) and visualized for different examples in Figs. 3(d)–3(g). With this approach, based on optically actuated micro-robotics, direct illumination by intense lasers on the trapping objects can be avoided so that tweezing materials of low damage threshold are facilitated.

III. TAILORED SCALAR LIGHT AS ADVANCED TRAPPING POTENTIALS

By projecting lenses and gratings in conventional HOT into the conjugated plane, multiple discrete Gaussian trapping potentials can be created from the initial beam. Therefore, multiple particles can be trapped and manipulated in 3D space. An alternative, advanced approach for creating multiple trapping sites is based on complexly structuring a scalar light field with a continuous intensity landscape, allowing a more versatile optical manipulation by a single structured beam. This approach benefits from the huge diversity of known scalar light fields, embedding additional properties as the transverse energy flow, optical angular momenta, attracting, accelerating, or non-diffracting characteristics.¹⁰

Scalar structured light fields include a spatially varying amplitude and/or phase distribution, whereby the polarization of light does not change in space. Nowadays, it is straightforward to shape these light

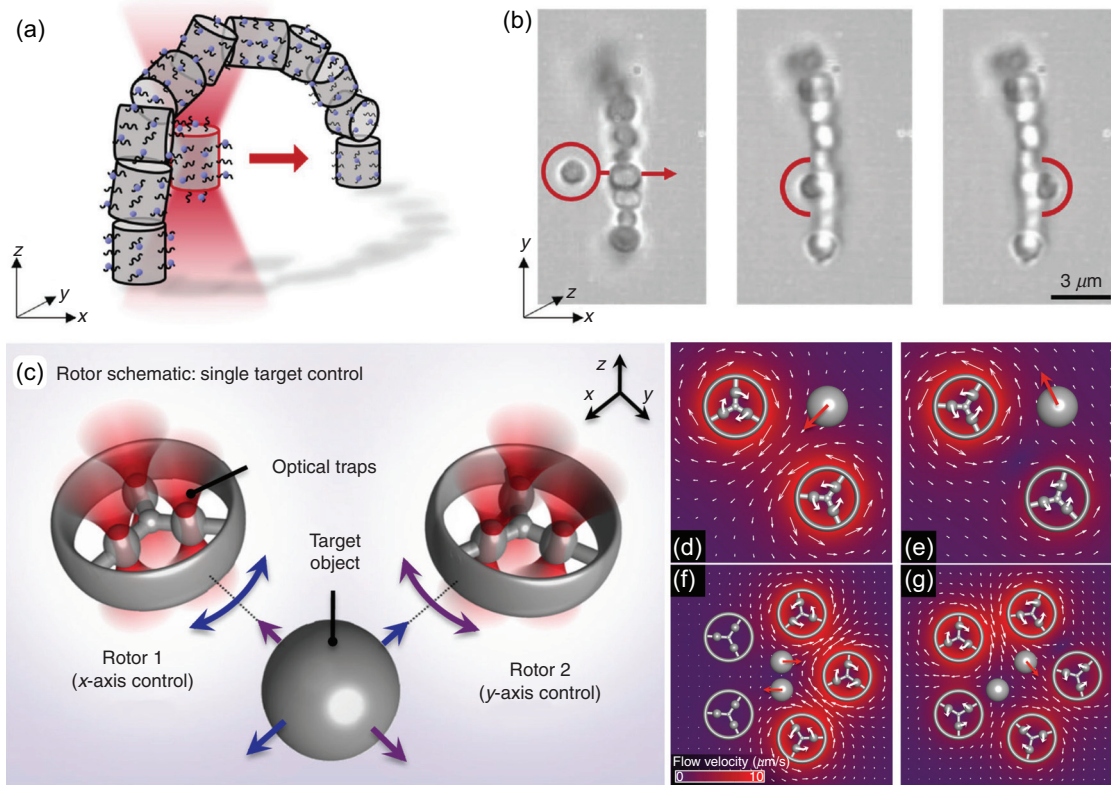


FIG. 3. Exemplary applications of holographic optical tweezers (HOT). Top: the realization of hybrid soft matter by zeolites with NH_2 -functionalized polymer brushes building an arch-type structure.⁸ (a) Barroso *et al.* assembled surface-functionalized nanoporous zeolite-L crystals by holographic optical tweezers to construct arbitrary 3D nanoarchitectures; (b) Shaped architectures remain permanently stable after release from the holographic optical tweezers system, as it is proven by guiding an unbound crystal (red circle) freely underneath the constructed arch from left to right [Adapted with permission from Barroso *et al.*, Part. Part. Syst. Charact. **35**, 1800041 (2018). Copyright 2018 Wiley-VCH Verlag GmbH & Co.].⁸ Bottom: HOT-driven micro-rotors for indirect optical trapping of absorbing particles;²⁸ (c) Rotor schematic for single target control; (d)–(g) different examples of guiding/enclosing absorbing objects by reconfigurable hydrodynamic manipulation. Adapted from Butaitė *et al.*, Nat. Commun. **10**, 1215 (2019). Copyright 2015 Author(s), licensed under a Creative Commons Attribution 4.0 License.²⁸

fields experimentally using, for instance, SLMs or DMDs (digital mirror devices).¹⁰ These devices may allow for amplitude or joint amplitude and phase modulation. The combined modulation facilitates arbitrary scalar light fields and is enabled by, e.g., a phase-only SLM. Following the ansatz of Davis *et al.*,²⁴ a weighted blazed grating approach is applied to encode not only phase ($\phi \in [0, 2\pi]$) but also amplitude ($A \in [0, 1]$, normalized) information in a phase-only hologram.^{24,51} When the desired light field (in the image plane of the SLM) is represented by $E = A \cdot \exp(i\phi)$, Davis *et al.* assumed the SLM transmission function to be $\exp(iA\phi)$. With the help of mixed Fourier–Taylor series, one can derive the required hologram

$$\Phi_h = A' \bmod[\phi + \phi_b - A'\pi, 2\pi], \quad (1)$$

generating E in its first diffraction order. Spatial separation of diffraction orders is realized by ϕ_b representing a blazed grating (with a periodic, spatially varying linear phase ramp). A' is the corrected amplitude function, with $\text{sinc}(1 - A') = A$. For details on this approach, the interested reader is referred to the respective Refs. 24 and 51.

In addition to holographic approaches based on SLMs or DMDs, there are various other methods to shape scalar light fields, representing

an own field of research. For instance, also static as well as tunable q-plates^{101,102} are established tools not only for amplitude and phase but also for polarization modulation (see Sec. V). Additionally, plasmonic or dielectric metasurfaces^{103–107} represent a continuously increasing research area, opening various innovative approaches for beam shaping. A thorough review of these topics is out of the scope of this manuscript. More details can be found in Refs. 108–110.

The ongoing advancement of modulation techniques still improves the already great accessibility of scalar structured light fields, so that a manifold of applications, including optical trapping, can benefit from it. In the following, we will concentrate on the light fields' intensity structure, giving an insight into how, in turn, realized scalar trapping potentials have allowed for the advancement of optical trapping.

A. From standard 2D to elegant 3D structured Gaussian potentials

Most established scalar structured light fields might be higher-order Gaussian modes, namely, standard Hermite–(HG), Laguerre–(LG), or Ince–Gaussian (IG) beams.^{111–113} These self-similar

light fields represent exact analytical solutions of the paraxial wave equation in Cartesian, polar, or elliptical coordinates, respectively. They do not change their extended transverse distribution significantly upon propagation, however showing divergence. This property makes them perfectly suited for optical trapping applications: on the one hand, their transverse intensity distribution does not change within the trapping volume. On the other hand, they can easily be generated by SLMs positioned in the conjugated (far field) or image plane of the trapping plane. The extended 2D transverse intensity structure of higher-order Gaussian modes makes them useful candidates for specialized potential landscapes. For instance, almost 30 years ago, the application of HG beams facilitated the alignment of non-spherical particles.³¹ Furthermore, the transverse 2D structure of LG modes or, more precisely, their collinear superposition allowed for size-selective trapping of spherical particles.³² Additionally, IG beams have been successfully used as complex continuous trapping potentials,¹¹⁴ enabling optical assembly of silica spheres into 2D microstructures. They also allow for 3D optical particle structures taking advantage of the self-similar propagation behavior of IG light fields combined with longitudinal optical binding.¹¹⁵ Particle chains are formed within the diverging light structure, since each particle acts similar to a spherical lens, confining light and, thereby, increasing gradient forces behind itself.

Recently, another, less prominent class of higher-order Gaussian trapping potentials has been introduced into the field of optical trapping: elegant Gaussian beams.^{116,117} These fields are complementary to standard self-similar Gaussian beams, as they show dynamic structural changes upon propagation, i.e., they are not only structured in 2D but even 3D space. In contrast to standard Gaussian beams, elegant Gaussian beams include a complex valued argument in the respective Hermite/Laguerre/Ince polynomials, resulting in an additional phase variation and, thus, in a modification of the usually spherical wave front of Gaussian beams.^{33,116} It has been demonstrated³³ that this class of Gaussian beams creates high gradient forces at small scales, being of special interest for trapping core-shell particles and nanocontainers.⁹ As illustrated in Fig. 4, Alpmann *et al.* compared the features of a fundamental Gaussian beam with those of elegant and a standard higher-order HG fields as trapping potentials for elongated particles. Depending on the chosen potential, dynamically realized by holographic beam shaping, different particle orientations are enabled. Structural changes of elegant HG modes in the propagation direction allow for enhanced trapping forces, revealing 3D structured scalar light fields as an innovative tool for advanced optical micromanipulation.

B. 3D particle control by tailored propagation of light

In addition to elegant Gaussian beams, there is a broad variety of scalar 3D structured light fields with tailored propagation behavior. Applying a single 3D structured light field, one can also optically manipulate particles in multiple transverse planes in 3D space simultaneously, enabling 3D particle assemblies. Even so-called tractor beams are facilitated, which allow attracting trapped particles against the scattering force, i.e., counter the beams propagation direction.

A well-known class of light fields shaped in 3D space is non-diffracting or propagation-invariant beams.¹¹⁸ In contrast to typically

diffracting beams as Gaussian light fields, non-diffracting fields are tailored to keep their transverse amplitude, phase, and polarization distribution unchanged for a specific propagation distance (“non-diffracting distance”). To realize this propagation behavior, all spatial frequency components in the far field of non-diffracting light fields are, in an ideal case, found on an infinitesimally thin ring around the optical axis. Each point on this ring creates a plane wave in real space, propagating under a defined angle to the optical axis. Simplified, the non-diffracting structure can be understood as the result of interference of these plane waves. Interestingly, these beams also “self-heal” if being partially disturbed by an obstacle:¹¹⁹ plane waves passing the object enable the self-reconstruction of the transverse field distribution after a corresponding shadow region of the obstacle.

One of the most established non-diffracting beam classes is the Bessel beam class exhibiting a ring-shaped transverse intensity profile, experimentally approximated by Bessel–Gaussian (BG) light fields.¹²⁰ In addition to this class of circular transverse symmetries, there are other classes as, for instance, Mathieu beams¹²¹ having a transverse shape belonging to the elliptical coordinate system, or the class of discrete non-diffracting light fields¹²² of custom transverse intensity distribution. The respective propagation-invariance and self-healing properties have proven to be valuable tools for simultaneous particle manipulation at different longitudinal *z*-distances and the 3D arrangement of micro-particles. In 2002, Garcés-Chávez *et al.* demonstrated the ability to apply a single first-order Bessel beam to simultaneously trap particles in the beams on-axis intensity maximum in two distant sample cells located in different (*x*, *y*)-planes, both within the non-diffracting distance of the light field.^{34,123} Although particles in the first cell disturb the trapping beam, the light field is fully reconstructed in the second cell, re-allowing for optical trapping. Combined with optical binding, even longitudinal particle chains are forming per cell. Beyond, Mathieu beams were implemented for 3D arrangements of spherical as well as non-spherical particles,³⁵ additionally considering more complex transverse intensity structures. Here, the ellipticity parameter and mode number as well as the choice between even, odd, and helical Mathieu beams allow for the on-demand adaption of transverse potential landscapes with multiple trapping sites, whereby the non-diffracting and self-healing property is kept.

Hence, scalar non-diffracting light fields allow for complex trapping potentials based on tailored transverse intensity structures propagating unchanged. However, on the basis of these non-diffracting beams, one is also able to design 3D trapping potentials additionally sculpted longitudinally as an optical tractor beam.³⁶ Ruffner and Grier have shown that, by coherently superimposing coaxial Bessel beams, a scalar light field of longitudinally periodic intensity variations can be realized. By holographic beam shaping via a SLM, the researchers demonstrated the entrapment of multiple particles in the maxima of the periodic intensity variation. Ruffner and Gier included a time-dependent relative phase shift between the superimposed beams by dynamically adapting the CGHs. By this approach, intensity maxima and, thus, trapped particles can be moved along the optical axis and counter to the direction of propagation, i.e., a conveyor (/tractor) beam is realized. Note that within the past few years, various different tractor beams have been designed, exclusively based on not only 3D structured light but also, e.g., the so-called optical pulling force and, therefore, specific particle parameters.^{124,125} A detailed review of the class of optical tractor beams and recent advances can be found in Ref. 126.

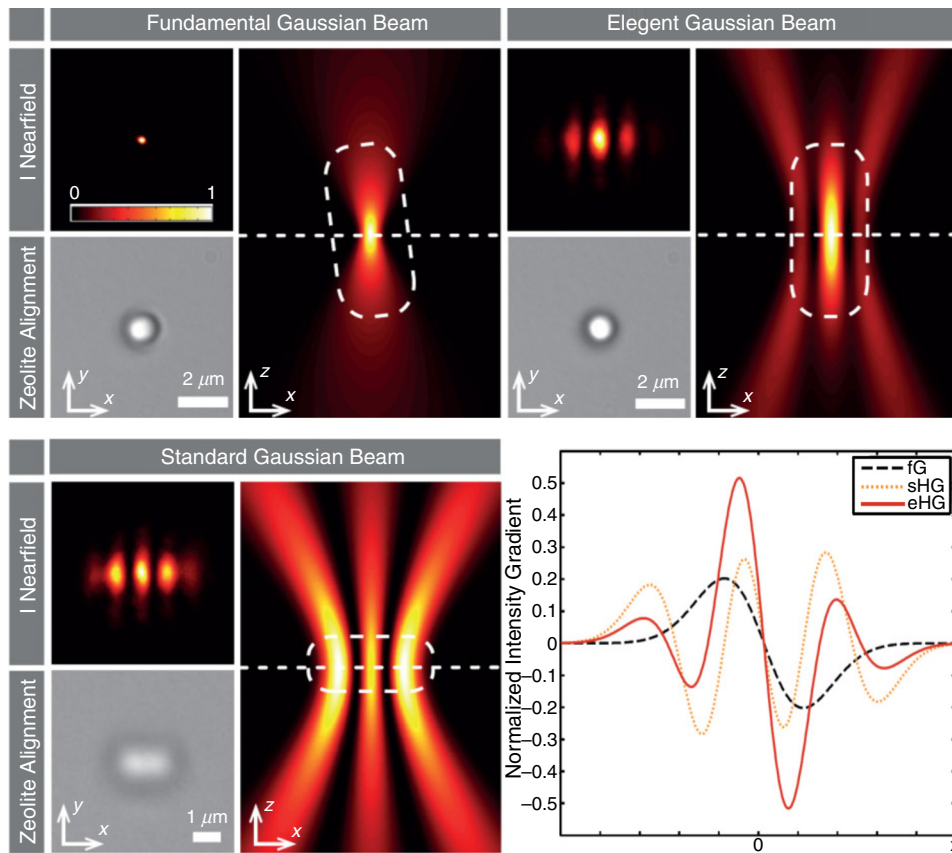


FIG. 4. Comparison between fundamental Gaussian, elegant HG, and standard HG beam (HG mode numbers: $n_x = 2$, $n_y = 0$) for optical alignment of elongated particles, namely, zeolite-L nanocontainers.³³ For each case, the transverse experimental intensity profile (top left), a bright field microscope image of the trapped particle (top view; bottom left), and a sketch of zeolite alignment in longitudinal intensity profile (right) are shown. The graph shows the intensity gradient $\nabla I / I_{\text{mean}}$ along the white dashed lines for each case. Adapted with permission from Appl. Phys. Lett. **106**, 241102 (2015). Copyright 2015 AIP Publishing LLC.³³

C. Intensity singularities in 3D caustic light fields

Another family of beams enriching the variety of 3D structured scalar beams are caustic light fields, known in ray optics for centuries.^{127,128} Caustics are an ubiquitous phenomenon in nature and everyday life, observable, e.g., when light is refracted in shallow water or a glass of wine.¹²⁸ They represent an envelope of a family of rays,¹²⁹ whereby their topology is classified by catastrophe theory via unique potential functions.^{128,130,131} Considered in theoretical ray optics, caustics correspond to intensity singularities of infinite intensity. In wave optics, the increase in intensity is finite but, however, shows a strong intensity gradient. Hence, caustic light fields are of specific interest for optical manipulation not only because they show a 3D varying spatial intensity structure but also due to strong intensity gradients, being related to strong optical forces.

A well-known example for caustic light is the Airy beam,¹³² realized experimentally for the first time in 2007.^{133,134} The Airy beam represents the optical analogon of a fold catastrophe and exhibits a curved propagation trajectory of its transverse intensity structure, as illustrated in Figs. 5(a) and 5(b). The curved trajectory is also followed by its propagating intensity singularity [intensity maximum in (a)], forming the caustic line [red line in (a) and (b)]. Because of this unique accelerating beam propagation, it is perfectly suited to realize an optical “snow blower,” as shown by Baumgartl *et al.* in 2008.³⁷ Figure 5(c) presents the principle of the implemented approach: the curved intensity structure of an Airy beam is used to push dielectric microparticles

by gradient and, in particular, scattering forces from one compartment into another.

Beyond Airy beams, a broad range of different caustic light fields were introduced the past few years, including Pearcey, swallowtail, or butterfly caustics.^{135–137} Also, these fields embed promising 3D characteristics for optical micromanipulation. For instance, the Pearcey beam shows, on the one hand, a curved trajectory, allowing for particle guiding on an s-shaped path.¹³⁸ On the other hand, tight confinement of light is found upon propagation without explicitly focusing, paving the way for enhanced gradient forces at the nano scale.

For moving trapped particles on the bent trajectory of a caustic light field, as exemplified by the optical snow blower, the Poynting vector, i.e., the energy flow of light, plays a major role. It defines not only the scattering force acting in the beam propagation direction but may also cause transverse movement of particles by its orbital or spin contributions. In the following, we outline the role of energy flow density and related optical angular momenta for optical trapping. Here, in addition to intensity, the beneficial properties of the two additional degrees of freedom of fully-structured light, namely, phase and polarization, become clear.

IV. ENERGY FLOW DENSITY AND OPTICAL ANGULAR MOMENTA

A. Fundamental properties

Bekshaev *et al.* give a detailed description of internal flows and energy circulation in light, which can be found in Ref. 49. Following

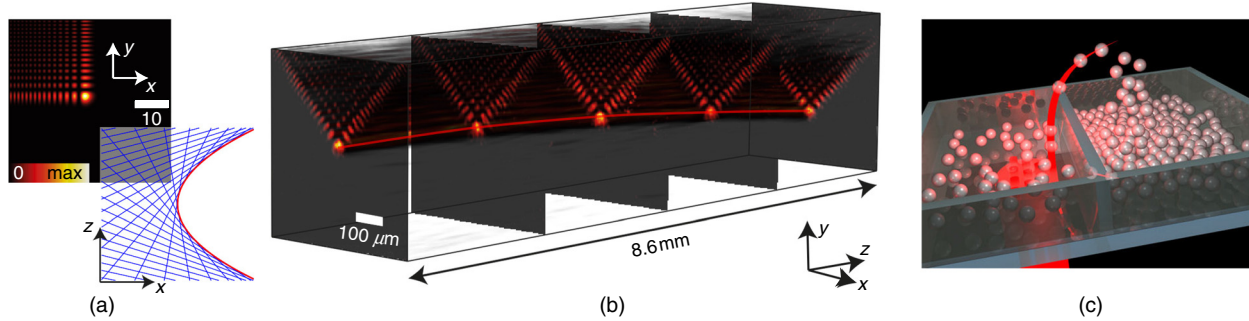


FIG. 5. Airy beam as an example of caustic light fields for optical micromanipulation: (a) transverse intensity structure (top) and corresponding rays [blue lines; (x, z) -plane] enveloping the parabolic caustic (red curve). Along this curved line, the transverse intensity structure propagates, as shown by holographically realized experimental images in (b). (c) Sketch of the Airy beam acting as optical snow blower of spherical particles. (a) and (b) Image courtesy of Alessandro Zannotti, WWU Münster, Germany. (c) Image courtesy of Kishan Dholakia, University of St. Andrews, UK.

their description, here, we give a short summary of terms being relevant for optical trapping.

Optical trapping and manipulation of particles are based on the momentum transfer of light with the momentum density given by^{49,139}

$$\vec{p} = \vec{S}_p / c^2. \quad (2)$$

Here, $\vec{S}_p \propto \vec{E} \times \vec{H}$ (\vec{E} and \vec{H} : electric and magnetic fields) represents the time averaged Poynting vector, giving the measure of the energy flow (or energy flow density) of light. Hence, Eq. (2) establishes the relation between Poynting vector and the dynamic attributes of light.⁴⁹ Furthermore, this relation, in turn, established the use of “momentum density” and “energy flow density” as synonymous terms.

For monochromatic light, the total energy flow can be written as the sum of its orbital and spin contributions (orbital and spin flow density, OFD and SFD), namely, $\vec{p} = \vec{p}_o + \vec{p}_s$, depending on the phase and polarization of light, respectively. The energy flow lines of the total energy flow as well as of its contributions are always continuous. However, integrated over the transverse (x, y) -plane, the spin contribution to the total beam momentum is zero.^{140–142} Note that, as the so-called “virtual” contribution to the energy flow, SFD was thought to be unmeasurable or non-observable¹⁴³ and does not exert force on absorbing Rayleigh particles. Based on these facts, researchers had mainly focused on studying the orbital (canonical) momentum density. However, the measurability^{143–146} as well as applicability¹⁴⁷ of SFD was demonstrated in 2014, increasing the interest in this originally virtual part.

Considered in the paraxial regime, the spin flow \vec{p}_s (SFD) is purely transverse, whereas the OFD \vec{p}_o also includes a longitudinal component.⁴⁹ In the following, we will concentrate on the transverse parts per unit z -length (linear momentum densities) in the paraxial regime, denoted as $\vec{P}_{(s,o)}$ with $\vec{P} = \vec{P}_o + \vec{P}_s$. We consider polarized, paraxial light $\vec{E} = [E_x, E_y]^T$ (Jones formalism) with $E_j = A_j \exp(i\phi_j)$, $j = \{x, y\}$. In this case, the orbital and spin parts of the energy flow are directly related to the phase ϕ and polarization handedness S_3 of light, respectively, with¹³⁹

$$\vec{P}_o = \frac{1}{k} (I_x \nabla \phi_x + I_y \nabla \phi_y), \quad \vec{P}_s = -\frac{1}{2k} (\vec{e}_z \times \nabla S_3) \quad (3)$$

and $\nabla = [\partial/\partial x, \partial/\partial y, \partial/\partial z]^T$, $I_j = |E_j|^2$, $\vec{e}_z = [0, 0, 1]^T$, wave number k , and the normalized Stokes vector¹⁴⁸ $\vec{S} = \vec{s}/s_0 = [S_0, S_1, S_2, S_3]^T$. The (normalized) Stokes vector is a typical way of

representing fully as well as partially polarized fields with $s_0 \in [0, 1]$ giving the intensity of light, $S_{1,2,3} \in [-1, 1]$ representing horizontal/vertical, diagonal/antidiagonal, or right-/left-handed circular states of polarization, respectively. Hence, S_3 defines the polarization handedness of the considered light field.

As visible from Eq. (3), for spatially structured phase $\phi(x, y)$ or polarization handedness $S_3(x, y)$, a spatial change in OFD or SFD, respectively, can be realized. The optical angular momentum of light is directly related to this energy flow and can be transferred in an optical trap to the captured object. It is $\vec{J} = \vec{L}_z + \vec{S}_z$ (Refs. 49 and 149) with orbital angular momentum \vec{L}_z (OAM) and spin angular momentum \vec{S}_z (SAM) given by⁴⁹

$$\vec{L}_z = \int \vec{r} \times \vec{p}_o \, d^2\vec{r}, \quad \vec{S}_z = \int \vec{r} \times \vec{p}_s \, d^2\vec{r}, \quad (4)$$

with \vec{r} being the spatial coordinate. Therefore, analogous to OFD and SFD, the OAM and SAM are dependent on the phase and polarization of light, respectively.

The SAM \vec{S}_z is associated with the polarization by a momentum of $\langle S_z \rangle = \pm \hbar$ per photon, with $+\hbar$ ($-\hbar$) corresponding to left-handed (right-handed) polarization as manifested by the sign of the S_3 Stokes parameter.⁴⁵ Taking advantage of the transfer of momentum, SAM has proven its benefit in, e.g., spinning trapped birefringent objects⁴⁸ in optical tweezers or sorting chiral particles due to the interaction of polarization handedness and particle chirality.^{150,151} In recent years, the question how to spatially structure SAM has become central with respect to the advance of tailored SFD structures. This will be discussed in more detail in Sec. V.

The OAM \vec{L}_z is determined by the spatial structure of light. For a phase vortex configuration $\exp(i\ell\varphi)$ [$\varphi \in [0, 2\pi]$: polar angle; cf. Fig. 1(d)], i.e., an azimuthally varying phase, the OAM is associated with $\langle L_z \rangle = \ell \hbar$ per photon.^{41,45,152,153} Here, ℓ describes the topological charge of the phase vortex, given by the change of phase (counter-clockwise) around the central point of undefined phase—a phase singularity—divided by 2π .^{127,154} Note that the topological charge represents the singularity index of the embedded phase singularity, around which the respective OFD rotates. It is well known that OAM carrying beams can be applied to orbit transparent particles around the optical axis or also spin absorbing particles enclosed in the beam’s dark center at the position of the phase singularity,^{42–44} as it was

already proven a quarter of a century ago. Today, there is a manifold of detailed reviews on OAM and its benefit for various applied fields of research, ranging from optical communication to high-resolution imaging (STED microscopy) and, obviously, optical manipulation (see, e.g., Ref. 155 and references therein). Hence, in the following we concentrate on giving an insight into innovative OAM structures in complex light fields and its use in applied optics by the example of optical metrology.

B. Customized phase flow

The probably best known example of OAM carrying light fields is self-similar helical LG beams, representing exact solutions of the paraxial wave equation in polar coordinates. Its transverse intensity structure shows concentric rings. The number and diameter of rings are defined by the radial mode index and topological charge, respectively.¹¹² In general, there is a broad variety of OAM beams being able to orbit or spin trapped particles. They embed the phase factor $\exp(i\ell\varphi)$ ($\varphi \in [0, 2\pi]$: polar angle) and, thus, the respective energy flow circulation around the central singularity. Another example for OAM beams, applied in optical trapping, is higher-order Bessel beams.¹⁵⁷ As LG beams, circular symmetric higher-order Bessel beams show a ring-shaped intensity structure with the number and diameter of the rings depending on the mode indices. However, while LG beams are self-similar, Bessel beams are propagation-invariant, belonging to the class of 3D structured, non-diffracting light fields (see Sec. III B). Hence, particles can be trapped in an longitudinally extended, non-diffracting volume. Recently, this property was also demonstrated in the so-called circular Airy vortex beams.¹⁵⁸ These beams impart OAM of charge ℓ and show a ring-shaped transverse intensity structure with an autofocusing, self-bending propagation behavior on parabolic trajectories.¹⁵⁸ Chen *et al.* applied these OAM beams to guide particles on curved trajectories in 3D space based on the beams' sophisticated propagation behavior. Additionally, such a beam allows to orbit trapped silica microparticles within the transverse circular intensity rings.

As visible from Eq. (3), phase-dependent energy flow \vec{P}_o does not necessarily require a circular symmetric field distribution as in LG, Bessel, or circular Airy vortex beams. Also light fields following elliptical coordinates can incorporate continuous phase flow topologies enabling the OFD, thus, OAM-dependent manipulation of particles. For example, self-similar helical IG beams or non-diffracting helical Mathieu beams, following the elliptical coordinate system, also carry an azimuthally varying phase structure¹⁵⁹ being related to transverse energy circulation.¹⁶⁰ Here, the transverse gradient of phase is spatially inhomogeneous, i.e., the phase does not increase linearly surrounding the optical axis. Therefore, the OFD varies spatially and the OAM per photon does not only depend on the topological charge ℓ , but particularly its ellipticity.^{160,161} This has been experimentally demonstrated by a slit diffraction-based metrology approach¹⁶⁰ and was also visualized based on nonlinear self-action of the light field in a nonlinear optical crystal.¹⁶²

Hence, the adaption of mode indices as the radial mode index, topological charge, or ellipticity of all light fields we presented until now enables the customization of energy flow for specific trapping applications. However, typically, the change of these mode indices is directly related to a change of the transverse extent of the intensity structure, which in turn represents a change in the trapping potential. Depending on the trapping application, such a change can be desired

but also unwanted. This change does not happen for an annular field profile with intensity distribution and radius both being independent of the topological charge ℓ of the embedded phase vortex. This property is provided by the so-called perfect optical vortex (POV) beams.^{163–165} In such a beam, the phase gradient (azimuthally linear) can easily be increased and, therefore, the strength of OAM/OFD enlarged, without changing the intensity profile, i.e., trapping potential landscape, first applied by Roichman *et al.* in 2007.^{163,164} Furthermore, this concept was implemented for optical trapping in 2013 by Chen *et al.*,¹⁶⁶ shaping respective fields by a combination of an axicon, a SLM, and a lens. By analyzing the rotation rate of particles trapped in POV beams of integer as well as fractional topological charge ℓ , Leach *et al.* experimentally verified the theoretical findings that the OAM per photon of a fractional vortex¹⁶⁷ is $\ell - \sin(2\pi\ell)/2\pi$. POV beams of fractional ℓ have also been a topic of interest lately: Tkachenko *et al.* applied particle rotation to analyze if the realization of perfect fractional vortex beams is fundamentally possible.¹⁶⁸ Furthermore, POV beams have also pioneered optical trapping and manipulating low-refractive-index particles, which is typically challenging due to strong repelling forces.¹⁶⁹ Liang *et al.* enclosed the low-refractive-index particle between an on-axis point trap and a surrounding quasi-POV beam, allowing for rotating the particle at ℓ -controlled speed.

Beyond, even light fields of tailored OAM fully independent of any mode indices can be shaped. For instance, Rodrigo *et al.* demonstrated the ability to customize light fields including their phase gradient along curves, even knotted geometries, in 3D space and applied created structures in optical trapping.^{170,171} Beyond, Rodrigo and Alieva introduced the so-called polymorphic beams and nature inspired energy flow circuits (see Fig. 6) as tailored tools for optical micromanipulation.¹⁵⁶ As indicated in Fig. 6(a), researchers presented a broad variety of accessible tailored fields including custom phase flow geometries (top: transverse intensity distribution; bottom: transverse phase structure). The respective OFD allows guiding particles on predefined trajectories in the trapping potential, as illustrated by the example in Fig. 6(b). Here, following the tailored OFD, particles are guided with spatially varying speed along a spiral-shaped intensity distribution.

C. OAM beams for optical metrology

Besides being used for guiding trapped particles, OAM-carrying light fields represent a valuable tool for optical metrology. In this case, the interaction of low-intensity OAM beam with particles, not being trapped, is applied. Advancing the field of optical activity, researchers demonstrated that the OAM of structured light can be used to enhance circular dichroism related to chiral molecules.⁴⁷ Furthermore, in laser remote sensing, a technique was proposed enabling the direct measurement of the transverse velocity component of a target by letting it interact with an OAM mode.^{46,172,173} For this purpose, the light scattered back from the target is detected, containing information about the target's position and velocity at each instant. For extracting the information, the scattered light is interfered with a reference beam. In 2015, Belmonte *et al.* implemented this OAM-based principle in fluid dynamics to measure the local vorticity of a flow,⁴⁶ by analyzing the light scattered from microparticles, as indicated in Fig. 7. Hence, structured OAM beams do not only advance optical trapping, but its low-intensity interaction with different objects as particles in fluidic systems or chiral molecules has opened up new perspectives in the field of optical metrology.

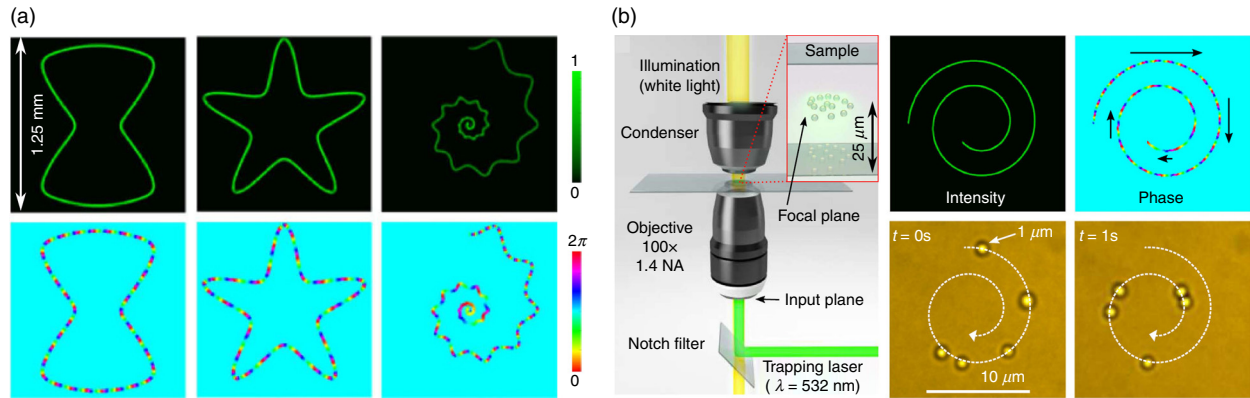


FIG. 6. Customized optical current in polymorphic beams.¹⁵⁶ (a) Examples of intensity (top) and phase (bottom) distribution of polymorphic beams (Fourier plane). The first example shows a constant phase gradient along the curve (constant $|\vec{P}_o|$), whereas the star and spiral structure embed a spatially varying gradient. (b) Application of Archimedean spiral beam of inhomogeneous phase gradient for manipulation of silica micro-spheres (left: setup sketch; top right: intensity/phase of trapping beam with arrows indicating strength of OFD; bottom right: bright field microscopy images of trapped and spiraled spheres). Adapted from J. A. Rodrigo and T. Alieva, *Sci. Rep.* **6**, 35341 (2016). Copyright 2015 Author(s), licensed under a Creative Commons Attribution 4.0 License.¹⁵⁶

V. VECTORIAL LIGHT AS A PIONEERING TOOL FOR OPTICAL MANIPULATION

As the third degree of freedom of fully-structured light, polarization can play a valuable role in optical micromanipulation. On the one hand, the polarization of light can be beneficial for handling polarization-sensitive objects, e.g., exciting responsive molecules in trapped nano-containers.¹⁷⁴ On the other hand, the polarization of light enables the transfer of SAM ($\pm\hbar$ per photon) to trapped objects^{48,150,151} as well as the creation of SFD (\vec{P}_s) topologies,¹³⁹ both depending on the polarization handedness $S_3 \in [-1, 1]$. Typically, the spin of light is applied via beams of spatially homogeneous polarization, although spatially structured polarization is a well-known

phenomenon for decades. It appears even naturally in the blue day-light sky.¹²⁷ Recent technical advances in light shaping methods have allowed customizing polarization. Thus, nowadays, it is straightforward to realize vectorial beams of inhomogeneous polarization as *vector fields* of linear polarization states varying in orientation or *ellipse fields*, which additionally include elliptical or circular states.¹⁷⁵ Within the latter, spatially varying S_3 , thus, SAM structures and complex SFD topologies can be realized. The accessibility of these vectorial beams opens new perspectives for optical trapping, especially since the measurability^{143–146} as well as applicability¹⁴⁷ of the virtual SFD part has been proven in different approaches. For instance, SFD can push and twist a probe Mie particle in an evanescent field.¹⁴⁷ Even though the spin contribution is typically orders of magnitude weaker than the radiation pressure force of the orbital part, this originally “virtual” property is attracting rising attention.

In the following, we will give an overview over different modulation approaches for shaping vectorial, i.e., polarization-structured light in the paraxial regime and detail how these techniques have been applied to spatially vary angular momenta or create spin flow topologies.

A. Superposition principle and customized SFD structures

A polarization-structured light field can typically be decomposed into two scalar fields E_u and E_v ($E_{u,v} = E_{u,v}^0 \cdot \exp(i\phi_{u,v})$) of orthogonal polarization following

$$\vec{E} = \vec{e}_u \cdot E_u + \vec{e}_v \cdot E_v. \quad (5)$$

Here, \vec{e}_u and \vec{e}_v represent two orthogonally polarized unit vectors ($\vec{e}_u \perp \vec{e}_v$; Jones formalism). Thus, at each point in space, the state of polarization of \vec{E} is defined by the local amplitude ($E_{u,v}^0 \in [0, 1]$) and phase ($\phi_{u,v} \in [0, 2\pi]$) relation between the scalar basis fields E_u and E_v .

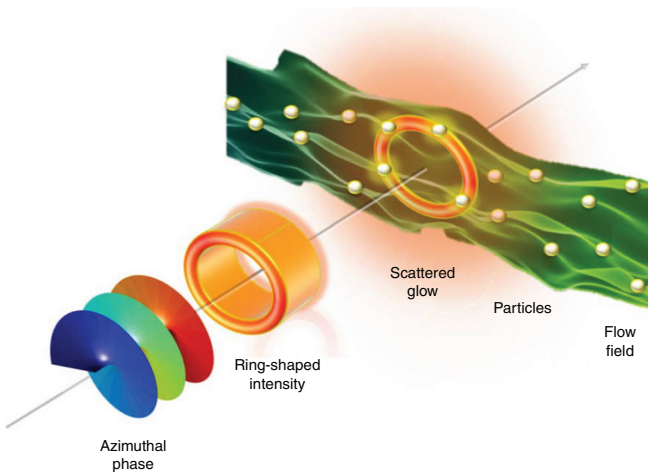


FIG. 7. Belmonte *et al.* implemented the orbital angular momentum (OAM)-based principle in fluid dynamics to measure the local vorticity of a flow, by analyzing the light scattered from microparticles, as indicated this figure. Reproduced with permission from Belmonte *et al.*, *Optica* **2**, 1002 (2015). Copyright 2015 The Optical Society.⁴⁶

Due to the diversity of scalar modes of light that can be used as basis states, various different vectorial light fields have been introduced. For instance, aiming at polarization-structured fields solving the vectorial Helmholtz equation in polar coordinates, helical LG or BG modes of orthogonal OAM and orthogonal polarization can be superimposed, resulting in cylindrical vector beams (CVBs)¹⁷⁶ or vector BG (vBG) beams,^{177–179} respectively. These classes include not only vector fields as radially or azimuthally polarized beams but also ellipse fields depending on the input beams' polarization. Moreover, by combining a fundamental Gaussian and a LG mode, full Poincaré beams¹⁸⁰ can be realized, including all polarization states of the Poincaré unit sphere. Beyond cylindrical symmetry, self-similar IG or non-diffracting Mathieu beams of elliptical/hyperbolic shapes allow forming complex polarization-structured fields, namely, Ince–Gaussian vector modes (IVMs)¹⁸¹ or Mathieu–Poincaré beams,¹⁸² respectively. When choosing the appropriate mode indices, the resulting vectorial beams inherit the propagation characteristics, as self-similarity, non-diffraction, and self-healing, of their scalar ancestors.^{178,179,181} Thus, the scalar mode indices as well as the input polarization states ensure a broad variety of adaptive polarization-structured fields.

Following the mathematical description of these light fields, a straightforward approach for their realization represents an interferometric system for the on-axis, co-propagating superposition of two

scalar, orthogonally polarized modes. Various different systems have been developed (see, e.g., Refs. 53, 183–193), enabling the superposition of mostly arbitrary scalar modes. The respective transformation of relative amplitude and phase differences into spatially varying states of polarization is best visible by the combination of a plane wave (polarization $\vec{e}_u = [0, 1]^T$) and a scalar structured field (polarization $\vec{e}_v = [1, 0]^T$),⁵⁰ as exemplarily shown in Fig. 8. Considering linear horizontal and vertical polarization as basis states, this approach results in a spatial polarization structure following $[E_v^0 \cdot \exp(i\phi_v), 1]^T$, directly determined by amplitude $E_v^0(x, y)$ and phase $\phi_v(x, y)$ (see Stokes parameters in Fig. 8). Researchers demonstrated that by this approach S_3 and, thus, the SAM are spatially shaped depending on $E_v^0(x, y)$ and $\phi_v(x, y)$, giving rise to complex, customizable SFD configurations.⁵⁰ Complex SFD topologies in ellipse fields can also be sculpted by various other combinations of scalar beams (e.g., Refs. 194 and 195), all opening new perspectives for particle manipulation by the energy flow of light. Beyond, these configurations are not only interesting for optical trapping or manipulation but also allow for the visualization of singular field properties: fix point within these energy flow configurations can be identified as polarization singularities (see Sec. V B) of the respective polarization structure.

Although interferometric approaches allow creating a broad variety of vectorial light fields and, thus, energy flow structures, their

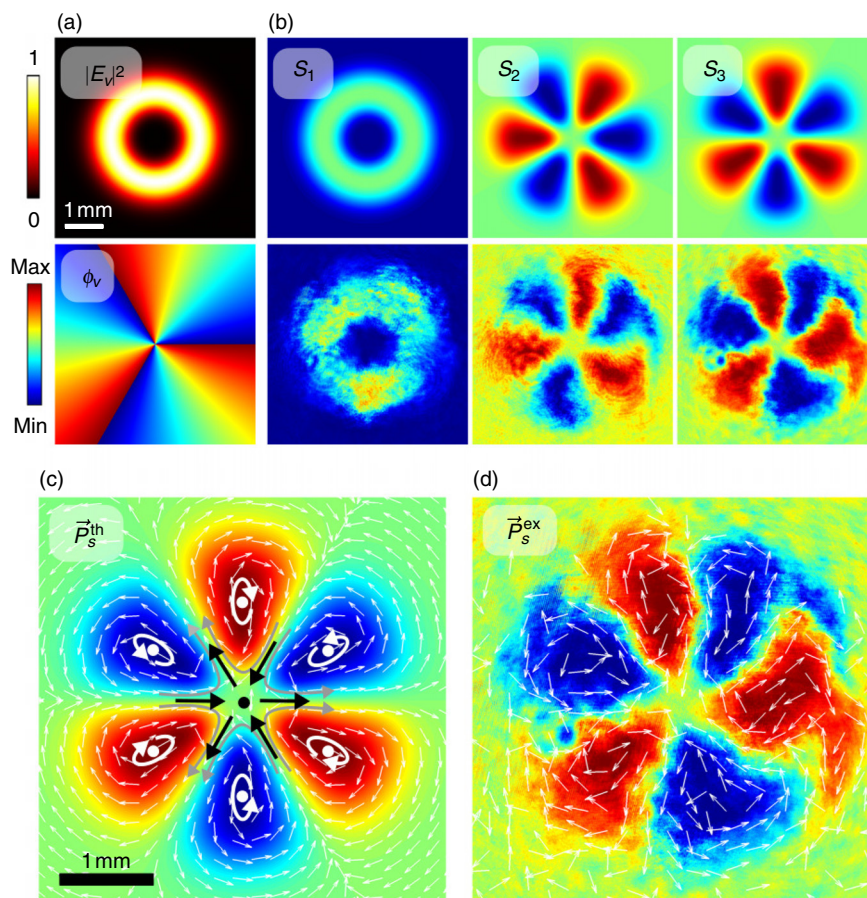


FIG. 8. Shaping SFD structures by an interferometric approach.⁵⁰ Combination of plane wave (E_u) and (a) scalar LG mode E_v results in a complex polarization structure [normalized Stokes parameters in (b), top/bottom: theory/experiment]. Spatially varying S_3 is directly related to custom SFD topology \vec{P}_s , illustrated in (c)/(d) (simulation/experiment). Arrows: SFD flow, white/black dots: centers/saddle points, background: S_3 . Adapted with permission from Otte *et al.*, J. Opt. **21**, 064001 (2019). Copyright 2019 IOP Publishing.⁵⁰

applicability is typically limited due to spatiotemporal inaccuracies caused by non-perfect on-axis superposition of combined beams. Tackling this issue, researchers developed more robust designs,^{190–193} e.g., by the reduction of optical elements.¹⁹³ Moreover, different single-beam approaches have been developed, avoiding issues of interferometric two-beam techniques. We exemplify these approaches in Sec. V B.

B. From single-beam approaches to fully-structured light

Single-beam methods are simplifying the realization of vectorial light fields. Among them, the so-called q-plates^{101,102} represent an established tool, consisting of a thin layer of liquid crystals between two glass plates, with a fast axis orientation forming a singular pattern of topological charge q . Depending on the polarization handedness, this plate can change the topological charge ℓ of a circularly polarized input beam by $\pm 2q$. Hence, a linearly polarized beam will be transformed into a superposition of two OAM beams of orthogonal circular polarization, i.e., a vectorial light field is shaped.^{179,196,197} Furthermore, also metasurfaces,^{189,198} intracavity approaches,¹⁹⁹ and gradient index lenses²⁰⁰ have been recently developed for the direct, robust realization of vectorial fields.

An even broader range of accessible vectorial light fields can be achieved by holographic shaping methods.^{51,52,55,184,186,201,202} Here, the common key element represents a SLM, which introduces a phase shift

between orthogonal polarization components of an incident light field. In this case, a digital hologram applied on the SLM determines the resulting polarization structure, allowing for on-demand beam shaping. For example, vectorial light fields embedding complex configurations of polarization singularity can be tailored, contributing to the topical field of singular optics.^{127,154} Therefore, before impossible studies on V-, C-, or L-singularities,¹²⁷ i.e., points or lines of undefined polarization, polarization orientation, or handedness, respectively, have been enabled. Figures 9(a) and 9(b) give two examples of holographically tailored vector fields, having a central, higher-order V-point singularity, characterized by the singularity index $\sigma_{12} = \oint d\Phi_{12}/2\pi = 4$ with $\Phi_{12} = \arg(\Sigma_{12})$, and complex Stokes field $\Sigma_{12} = S_1 + iS_2$.¹⁷⁵ The surrounding vectors typically form flower- ($\sigma_{12} > 0$) or web-structures ($\sigma_{12} < 0$) dependent on the sign of the singularity index.^{202,203} It has been shown that the position, number, and index of embedded singularities as well as the shape of surrounding light field can be customized by the SLM and wave plates.^{52,202}

In addition to pure polarization modulation, some of the approaches described can even combine the independent customization of amplitude, phase, as well as polarization (e.g., Refs. 52, 55, 186, and 205). Thus, fully-structured fields^{54,55} can be shaped, enabling the realization of customized optical trapping potentials. In particular, the combination of spatially structured OAM and SAM paves the way for advanced optical trapping with customized optical angular momenta. Figures 9(c) and 9(d) show a recent example, in which Alpmann *et al.* realized an OAM-carrying light field with a ring-wise variation of SAM.⁵²

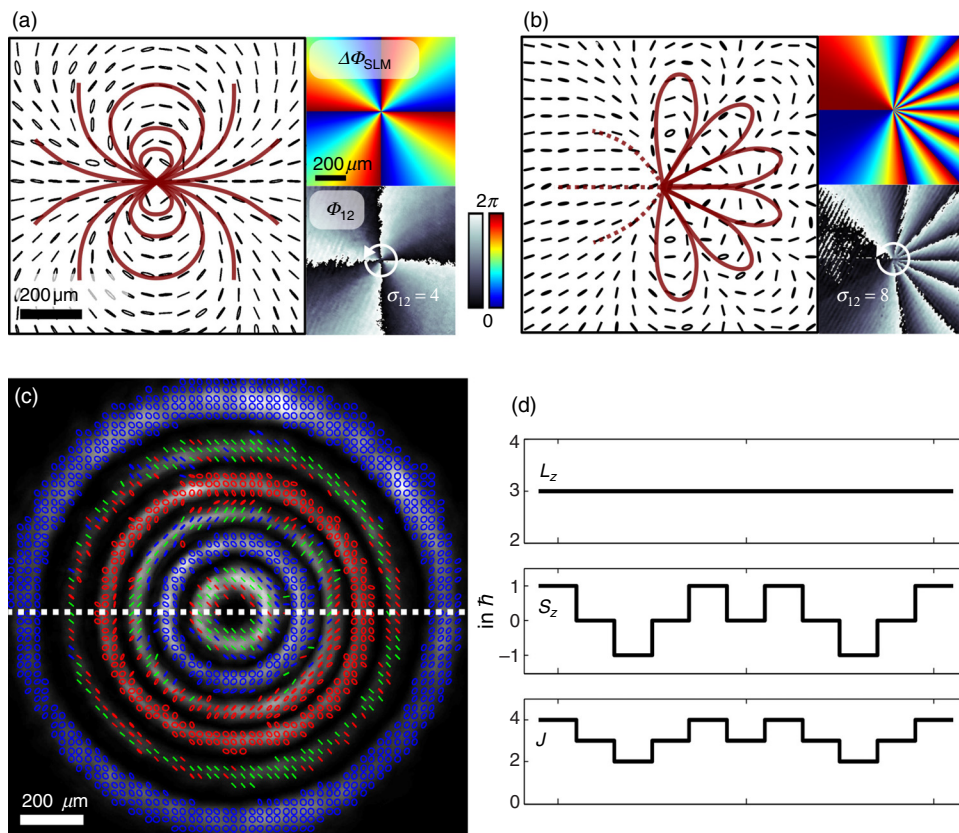


FIG. 9. Holographic customization of vectorial light. (a) and (b) Vector fields of flower shape tailored by a combination of the SLM ($\Delta\Phi_{\text{SLM}}$: SLM hologram) and quarter wave plates,²⁰² embedding a higher-order central V-point identified as Φ_{12} phase singularity (black lines: polarization states, red: flow lines). Adapted with permission from Otte *et al.*, J. Opt. 18, 074012 (2016). Copyright 2016 IOP Publishing.²⁰² (c) Fully-structured light field including tailored amplitude, phase, and polarization.⁵² Here, the light field carries OAM of a helical LG mode ($\ell = 3$) as well as a ring wise variation of polarization handedness, thus, SAM. The transverse variation of OAM, SAM, and total angular momentum (per photon) along white dashed line is shown in (d). Adapted from Alpmann *et al.*, Sci. Rep. 7, 8076 (2017). Copyright 2015 Author(s), licensed under a Creative Commons Attribution 4.0 License.⁵² Polarization is analyzed by spatially resolved Stokes polarimetry.^{202,204}

C. Shaping polarization in 3D space

Until now, mainly transverse structures of polarization, its customization, and analysis have been investigated. However, recently, due to vastly improving the ability to shape polarization on demand, the 3D propagation behavior of light can be accessed. Considering, for instance, the 3D optical manipulation of polarization-sensitive objects, the expansion of trapping volumes, or the customization of fully-structured light for elongated particles, the importance of 3D structured polarization becomes clear.

As described in Sec. V A, based on the superposition principle, one can realize vectorial light fields inheriting the propagation behavior of its scalar ancestor. For instance, by combining scalar propagation-invariant BG or Mathieu fields with an appropriate choice of mode indices, the formation of non-diffracting, self-healing vector Bessel–Gaussian (vBG) or Mathieu–Poincaré fields, respectively, is facilitated.^{177–179,182} Moreover, it has been shown that vBG fields of transversely homogeneous, but longitudinally inhomogeneous or transversely as well as longitudinally inhomogeneous states of polarization can be shaped²⁰⁶ based on a transverse-to-longitudinal modulation strategy.²⁰⁷

However, 3D structured polarization is not limited to fields based on non-diffracting beams: researchers demonstrated the ability to sculpt 3D varying polarization distributions based on the fundamental concept of counter-propagation.^{53,208,209} Therefore, orthogonally polarized LG or CVBs were combined, enabling significant changes in polarization within propagation distances of a wavelength. Within the study of counter-propagating CVBs of orthogonal polarization, revealing entanglement beating,⁵³ Otte *et al.* also found paraxial spin-orbit-coupling in free space. This behavior of SAM and OAM is of topical interest, recently studied in more detail by Li *et al.*²⁰⁹ who elucidated the role of orbit-orbit and spin-spin interaction between the

electric and magnetic fields. Figure 10 explains the pioneering result of Otte *et al.*, showing counter-oscillating spin and orbital angular momentum upon propagation. Light fields including this custom property are of specific interest for 3D optical manipulation in a counter-propagating trapping configuration, as they enable the orbiting/spinning of trapped objects only in scalar planes, whereas in purely vector planes no effect of angular momentum is expected.

VI. FOCAL FULLY-STRUCTURED TRAPPING LANDSCAPES

Structured light is not only important due to its valuable on-demand OFD and SFD characteristics: it gets especially interesting if we tightly focus (numerical aperture $NA \geq 0.7$) structured light of specific phase/OAM or polarization/SAM properties. When changing from the paraxial to the non-paraxial regime, significant longitudinal polarization components are formed in addition to typical transverse field components in the focal light field; thus, $\vec{E} = [E_x, E_y, E_z]^T$. These fields embed specific non-paraxial properties, being of utmost interest for optical trapping, in which tightly focused fields are frequently used. For instance, in the non-paraxial regime, the division of energy flow into S_3 -dependent spin and ℓ -dependent orbital parts is no longer valid.^{210,211} Furthermore, the conversion from SAM to OAM is found,^{212–215} which can alternate the orbital rotation speeds of trapped particles, as proven experimentally.²¹⁵ This conversion is still of topical interest: recently, Arzola *et al.* demonstrated that spin-orbit interaction by tight focusing gives rise to series of subtle, but observable, effects on the dynamics of a trapped dielectric micro-sphere.²¹⁶

One of the most powerful advancements is the implementation of polarization-structured light as the initial beam, allowing for fully-structured focal light, innovative custom trapping landscapes, until now unexploited trapping forces, complex 3D instead of typical 2D

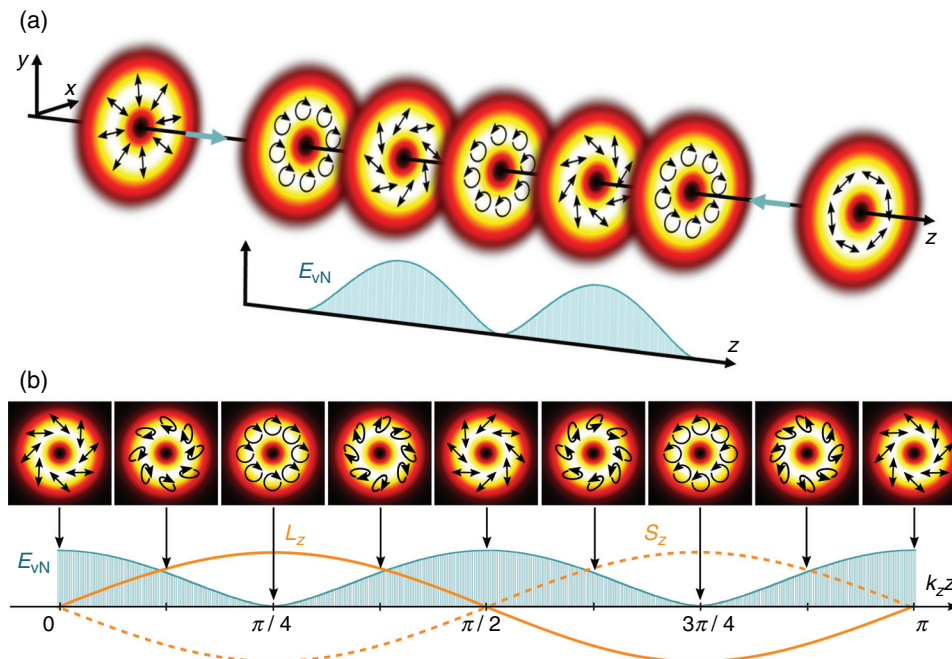


FIG. 10. Paraxial spin-orbit coupling in free space.⁵³ (a) The counter-propagating superposition of orthogonally polarized CVBs results in a 3D structured vectorial light field of oscillating vectoriness. (b) The graph (bottom) illustrates the corresponding variation of the von Neumann entanglement entropy upon propagation (classical consideration, $E_{vN} \in [0, 1]$) which is maximal/minimal for the vector/scalar field distribution (top: intensity and polarization). SAM (dashed orange line) and OAM (solid orange line) are counter-oscillating upon propagation, revealing paraxial spin-orbit coupling in this free-space configuration. Adapted from Otte *et al.*, *Light Sci. Appl.* 7, 18009 (2018). Copyright 2015 Author(s), licensed under a Creative Commons Attribution 4.0 License.⁵³

polarization states and topologies, and many more. In the following, we will give an insight into these cutting-edge innovations enabled by sculpted polarization.

A. Basic vector fields for optical trapping

If a polarized light field is tightly focused, initial radial polarization components will be tilted, forming significant longitudinal focal field contributions, whereas azimuthal electric field components stay unaffected (see Fig. 11). It has been shown that this behavior already makes basic vectorial light fields (first-order vector beams, $|\sigma_{12}| = 2$), namely, radial and azimuthal (cylindrical) vector beams, attractive for optical single-beam trapping: a purely radially polarized vector field enables the realization of a tighter focal spot.⁵⁷ Compared to a linearly polarized trapping beam, this focusing behavior of radial beams results in a larger axial, but smaller transverse trapping efficiency.²¹⁷ Thus, the general performance of optical tweezers can be improved due to reduced scattering forces.⁵⁹ Comparing the basic vector to Gaussian beams, Zhong *et al.* revealed higher axial trapping forces on core-shell magnetic microparticles for both radial and azimuthal fields.²¹⁸ In addition, it has been shown that azimuthal beams exhibit stronger lateral trapping forces than radially polarized ones.^{60,219} Based on these findings, Moradi *et al.* recently studied the influence of the numerical aperture, spherical aberration, and particle size on the trapping stiffness of radially, azimuthally, and linearly polarized

beams.²²⁰ Beyond, in 2019, Li *et al.* have shown that the tightly focused vector beam can exert chirality-tailored optical forces, enabling the selective trapping and rotation of small chiral particles.²²¹

To achieve further advancement of these applications, researchers recently focused multiple basic vector and scalar fields in a joint trapping plane,⁵⁸ shaping an array of higher-order Poincaré sphere (HOPS) beams²²² ($|\sigma_{12}| = 2$, $|\ell| = 1$) as input. More precisely, Bhebhe *et al.* designed a vector HOT⁵⁸ (see Fig. 12)—the further development of standard HOT (see Sec. II). To realize HOPS beams based on the superposition principle (see Sec. V A), the according hologram carries the spatially multiplexed information of all imparted scalar modes, following the group's former presented approach to realize multiple vector beams by a single SLM.¹⁸⁷ Subsequently, realized HOPS beams are tightly focused. In addition to other combinations, Bhebhe *et al.* combined a radial, an azimuthal vector, and a linearly polarized OAM beam in the trapping plane.

B. Focal field customization by polarization modulation

In addition to implementing multiple beams to form a complex trapping landscape, advanced polarization customization of a single input beam, also combined with amplitude and/or phase modulation, represents another innovative way to create trapping potentials. These may embed, e.g., custom 3D intensity distributions, 3D polarization

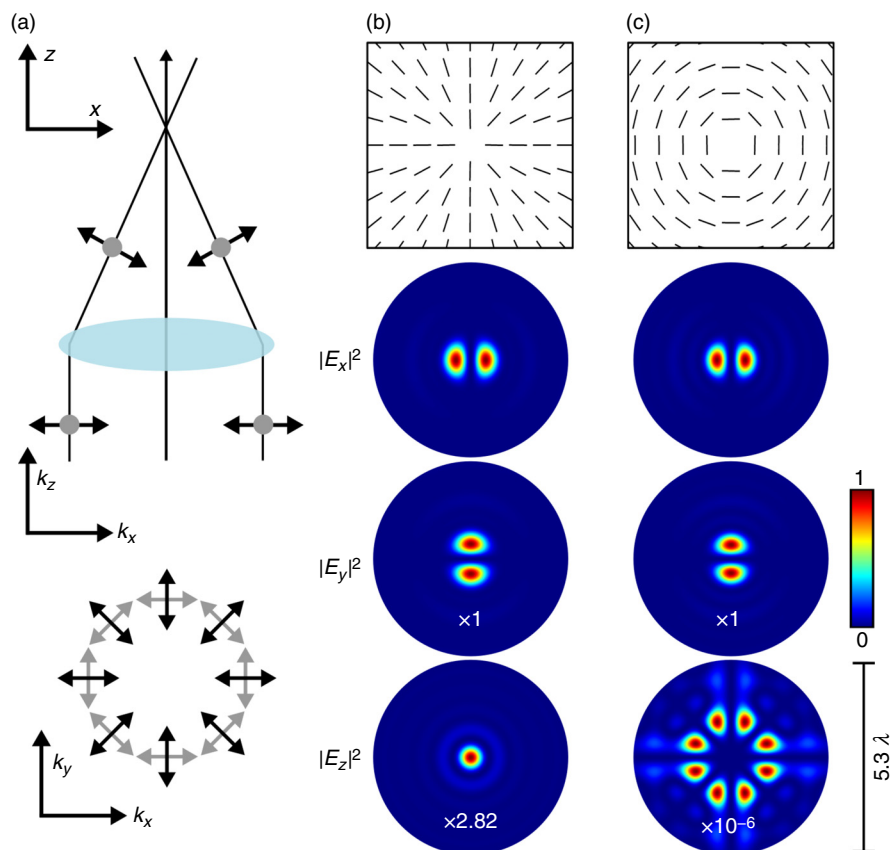


FIG. 11. Tight focusing properties of vectorial light. (a) Concept of the realization of longitudinal focal field contributions by initial radial components (black arrows), while azimuthal components stay unaffected (gray arrows/dots; wave vector $\vec{k} = [k_x, k_y, k_z]^T$). (b) and (c) Focal intensity contributions $|E_{x,y,z}|^2$ for focusing a purely (b) radial and (c) azimuthal vector field (top: transverse input polarization; NA = 0.9). The ratio of the maximum of $|E_{y,z}|^2$ to the one of $|E_x|^2$ is given within respective images.

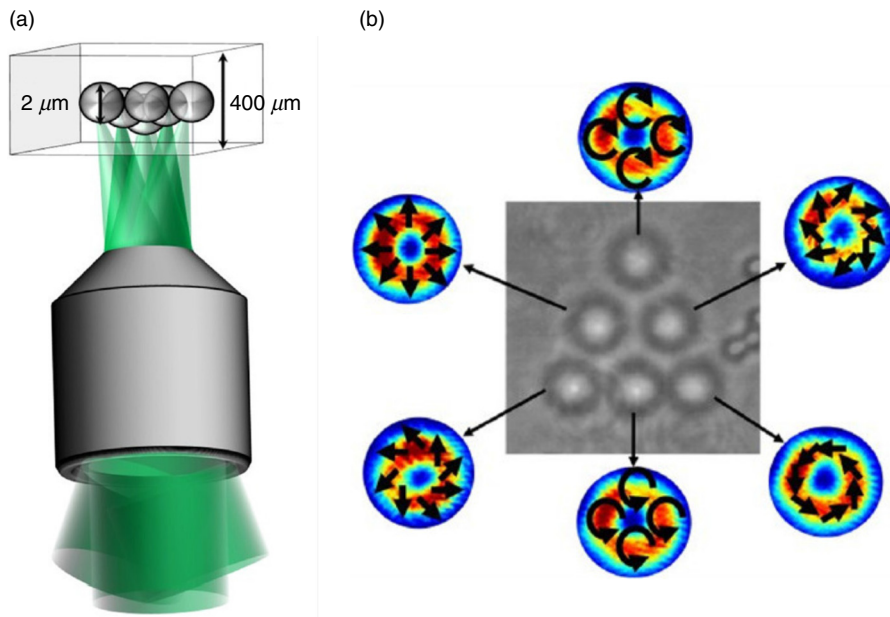


FIG. 12. Vector HOT enabling the dynamic implementation of multiple HOPS beams for particle manipulation.⁵⁸ (a) Scheme of developed vector HOT used for trapping dielectric 2 μm -particles. (b) Experimental image of trapped particles (top view) with insets of transverse intensity and polarization of applied HOPS beams (non-focused distributions). Adapted from Bhebhe *et al.*, Sci. Rep. 8, 17387 (2018). Copyright 2015 Author(s), licensed under a Creative Commons Attribution 4.0 License.⁵⁸

topologies, and/or energy flow configurations. For instance, different researchers combined the initial radial or azimuthal vector fields with specific diffractive optical elements before tight focusing, enabling the formation of an optical bubble,^{61,224} optical needle,^{225,226} or optical chains of voids²²⁷ within the focal intensity structure. Additionally, it has been demonstrated that these basic vector fields can be applied in combination with, e.g., sector-shaped obstacles⁶³ or annular vortex phase masks²²⁸ to shape the corresponding energy flow in the focal field.

Going beyond focusing basic vector fields, recently, Li *et al.* implemented a tightly focused vectorial beam with radially varied states of polarization to allow enantioselective optical trapping of chiral nanoparticles in spatially separated locations.²²⁹ In this case, a double focus of specific chirality-sensitive properties was shaped, taking advantage of the ability to tailor the focal trapping landscape dependent on polarization customization of the input field.

To enable a controlled realization of focal intensity landscapes, singular light fields with a central singularity ($|\sigma_{12}| \geq 2$) are

the structures of choice. For instance, tightly focusing higher-order vector fields²⁰² of index $|\sigma_{12}| > 2$ results in characteristic transverse intensity distributions depending on the sign of the central singularity's index.⁶² More precisely, dark stars or bright flowers are shaped for positive or negative input indices, respectively. A direct relation between input singularity index and the resulting number of star points or flower petals facilitates the controlled formation of focal intensity landscapes. This customization can even be advanced by adding a phase vortex to the electric input field. This enlarges the range of accessible intensity, thus, trapping landscapes,²²³ enabling the tuning of the focal field according to the trapping object, as exemplarily illustrated in Fig. 13. The focal field intensity can be adapted so that an elongated nano-container is stably aligned with the optical axis [see (b) and (c) $\ell = 3$]. Additionally, the customized 3D polarization is of similar interest as the intensity for trapping nano-containers that embed polarization sensitive, responsive molecules. The respective focal field can

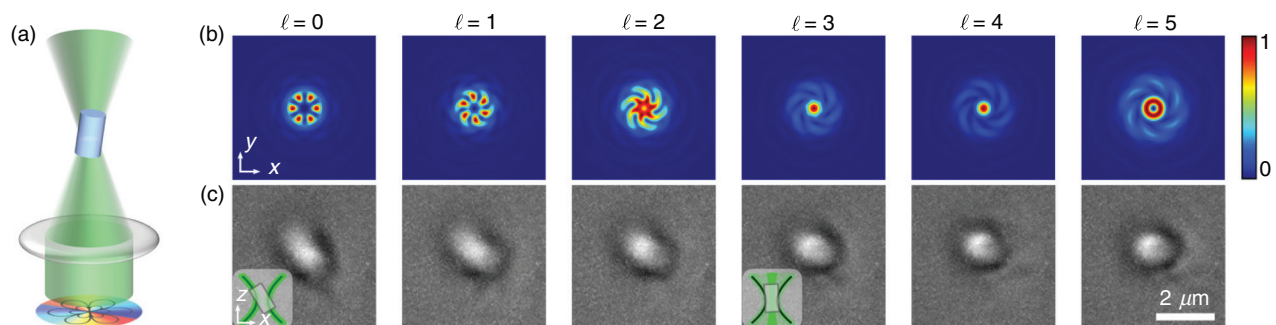


FIG. 13. Exemplary trapping of cylindrical zeolite-L nano-containers by higher-order vector field ($\sigma_{12} = 8$) with additional phase vortices of charge ℓ ($NA = 1.4$, oil immersion objective, zeolites in water, trapping wavelength $\lambda = 532 \text{ nm}$). The trapping concept is shown in (a). By implementing phase vortices, the (b) transverse intensity distribution (normalized) can be tuned, influencing (c) the zeolite orientation (top view; insets indicate orientation). Note that focal fields can have valuable 3D polarization properties: for $\ell = 3$ strong longitudinal field contributions are found,²²³ which could be applied to excite polarization sensitive molecules aligned in the channels of the zeolite (along the long axis).

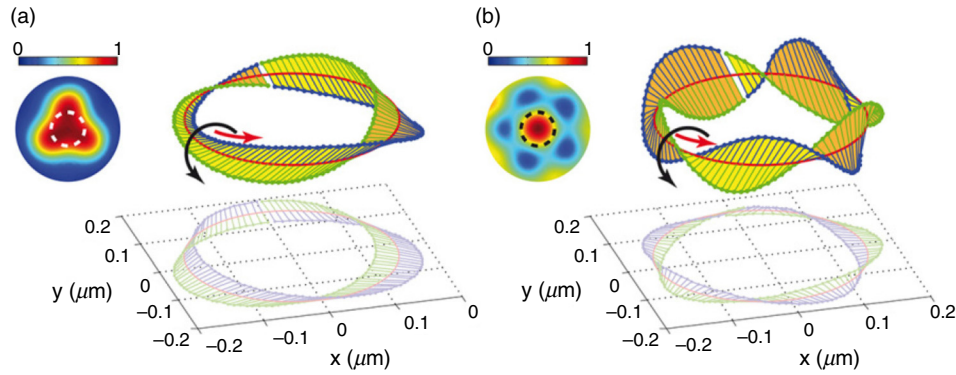


FIG. 14. Optical polarization Möbius strips shaped by tightly focusing CVBs⁶⁵ (experimental results). CVBs are formed by (a) $q = 1/2$ - and (b) $q = 3/2$ -plates, and the focusing objective has a NA of 0.9. Major axes of 3D polarization ellipses are traced on a circle located in the focal plane around the optical axis (see the white dashed circle in insets of focal intensity distribution). One half of the major axes are colored blue, while the other half is colored green for improved visualization. Reproduced with permission from Bauer *et al.*, *Science* **347**, 964 (2015). Copyright 2015 The American Association for the Advancement of Science.⁶⁵

be simultaneously applied for trapping as well as excitation of loaded molecules by its polarization topology. In the presented case, for $\ell = 3$ the focal field embeds strong longitudinal field components,²²³ which could excite molecules arranged along the zeolite's long axis.

C. 3D polarization topology, its analysis and future potential

Non-paraxial fully-structured fields may also include complex topologies as optical cones, ribbons, and Möbius strips. These have already been predicted in 2005 by Freund⁶⁴ and were proven

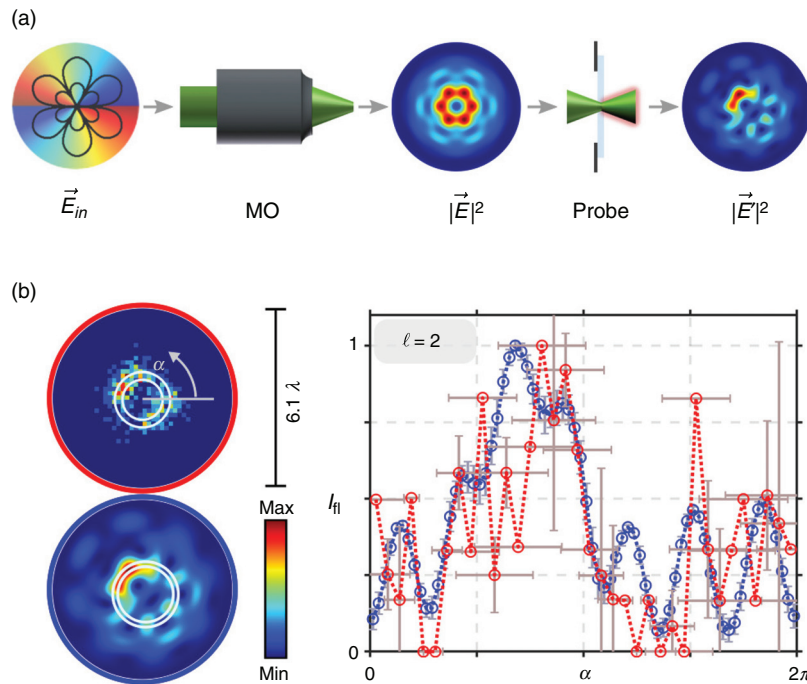


FIG. 15. Single-shot identification by the nanotomographic approach based on the self-assembled responsive monolayer.²²³ (a) Concept of the measurement procedure (\vec{E}_in : input electric field, MO: microscope objective, $|\vec{E}|^2$: normalized transverse focal field intensity, probe: fluorescent monolayer on glass, $|\vec{E}'|^2$: normalized transverse intensity of fluorescent response). (b) Exemplary measurement results for tightly focused (NA = 0.8) vector field with $\sigma_{12} = 8$ and additional phase vortex of charge $\ell = 2$. Left: experimental/theoretical fluorescence distributions (red/blue). Right: intensity values within ring-shaped subspace of detected transverse fluorescence dependent on angular position (cf. white rings in left images; red/blue: experiment/simulation). Adapted from Otte *et al.*, *Nat. Commun.* **10**, 4308 (2019). Copyright 2015 Author(s), licensed under a Creative Commons Attribution 4.0 License.²²³

experimentally 10 years later by Bauer *et al.*⁶⁵ Figure 14 illustrates respective experimental results realized by tightly focusing a CVB shaped by a q-plate of charge (a) $q = 1/2$ and (b) $q = 3/2$. Here, the major axes of 3D polarization ellipses are traced on a circle (white dashed circle in insets of total focal intensity), forming the 3/2- and 5/2-twist Möbius strip. The circle is located in the focal plane ($z = 0$) around the optical axis. Since this experimental proof, the range of studied complex topological structures, especially Möbius configurations, has increased significantly, not only realized by tight focusing.^{66,230–234} For instance, researchers demonstrated the creation of optical Möbius strips with exotic twisting behavior,²³¹ analyzed Möbius strips around points of purely transverse spin density,²³⁵ and realized extended arrays of Möbius strips around focal singular points of adaptable number and index.⁶⁶

Customized 3D topological structures are pioneering the optical fabrication of novel functional media based on non-trivial topologies or the assembly of polarization-sensitive particles. For example, implementing custom polarization topologies, polarization-sensitive nano-objects can be arranged in order to form novel functional chiral metasurfaces by bottom-up assembly.

For those next-generation applications, the experimental analysis of focal fully-structured light fields is essential. However, due to their nano-scale details as well as their 3D polarization nature, methods typically applied in the paraxial regime are not applicable for the non-paraxial analysis. Hence, within the past few decades, researchers intensively worked on detection methods.^{223,236–238} For instance, Bauer *et al.* presented an approach based on scanning the focal field by a scattering gold nano-particle, enabling the measurement of focal amplitude, phase, and 3D polarization with high precision²³⁸ (see Fig. 14). Going beyond scanning the field of interest, a nano-tomographic method²²³ has been developed, allowing for the single-shot identification of focal fields and their non-paraxial properties. This method is based on the implementation of a responsive nano-system, more precisely, a self-assembled monolayer of fluorescent molecules, with a response depending on focal amplitude, phase, and 3D polarization. The respective working principle is illustrated in Fig. 15. These emerging methods now enable the detailed analysis of customized non-paraxial light fields and, thereby, advance the implementation of future optical trapping and manipulation applications.

VII. CONCLUSION

Although optical trapping is established in the optics community for already half a century, the pace of innovations is still unchanged. In particular, the implementation of structured light, which has led to path-breaking inventions in, e.g., high-resolution microscopy or optical communication, has unveiled a huge unexploited potential for optical trapping. On the one hand, scalar beam shaping has enabled HOT, advanced trapping potentials by light fields, which are 2D or even 3D sculpted in amplitude and phase, and the transfer of tailored OAM/orbital energy flow on trapped objects. On the other hand, recent advancement in polarization modulation has opened up a whole new class of light fields for optical manipulation: vectorial and fully-structured beams. Customized spin angular momentum, trapping potentials tailored for polarization-sensitive particles, and 3D extended vectorial fields embedding a not yet exploited kind of paraxial spin-orbit-coupling will pave the way for next-generation trapping applications. Beyond, the topical, still emerging field of tightly focusing scalar, vectorial, or fully-structured light fields reveals the ability to tailor

focal trapping potentials, trapping forces, energy flow, and 3D polarization topologies, among others. Recently studied innovative non-paraxial light fields may enable, for instance, the formation of novel functional media as chiral metasurfaces by light-assisted bottom-up assembly of polarization-sensitive or -responsive objects taking advantage of, in particular, the 3D polarization of structured non-paraxial light.

Optical trapping by structured light has also recently spread in various related fields: in 2019, the holographic acoustic tweezers (HAT) was introduced,²³⁹ based on the principle of HOT. Additionally, SAM and OAM in acoustic beams were studied,²⁴⁰ and an acoustical equivalent of an OAM beam, orbiting trapped objects, was created.²⁴¹ Furthermore, plasmonic effects are implemented for strengthening optical trapping and binding of nano-particles²⁴² or for the realization of nano-aperture tweezers with light shaped at the nano-scale to manipulate nano-particles or analyze viruses, DNA fragments and proteins,^{10,243,244} and tightly focused vectorial light fields allow for plasmonic trapping of metallic particles.²⁴⁵ Moreover, also atom trapping follows the example of implementing structured light; for instance, in 2018 Selyem *et al.* studied the shaping of atomic populations using a near resonant laser beam with a holographically controlled 3D intensity profile.²⁴⁶ Furthermore, using a DMD, in 2016 Gauthier *et al.* shaped the configurable microscopic optical potential for the trapping of a Bose–Einstein condensate.²⁴⁷ Hence, structured light not only has found its way into the field of optical trapping, coming along with continuing progress, but also significantly advances applied research fields as acoustic, plasmonic, and atomic trapping.

ACKNOWLEDGMENTS

The authors acknowledge partial support from the German Research Foundation (DFG), under Project No. DE-486/23-1, as well as by the European Union (EU) Horizon 2020 program, in the Framework of the European Training Network ColOpt ITN 721465.

DATA AVAILABILITY

The data that support the findings of Figs. 11 and 13 are available from the corresponding author upon reasonable request.

REFERENCES

- A. Ashkin, “Acceleration and trapping of particles by radiation pressure,” *Phys. Rev. Lett.* **24**, 156 (1970).
- A. Yao, M. Tassieri, M. Padgett, and J. Cooper, “Microrheology with optical tweezers,” *Lab Chip* **9**, 2568–2575 (2009).
- M. Fischer, A. C. Richardson, S. N. S. Reihani, L. B. Oddershede, and K. Berg-Sørensen, “Active-passive calibration of optical tweezers in viscoelastic media,” *Rev. Sci. Instrum.* **81**, 015103 (2010).
- M. Tassieri, F. Del Giudice, E. J. Robertson, N. Jain, B. Fries, R. Wilson, A. Glidle, F. Greco, P. A. Netti, P. L. Maffettone *et al.*, “Microrheology with optical tweezers: Measuring the relative viscosity of solutions at a glance,” *Sci. Rep.* **5**, 8831 (2015).
- M. L. Bennink, S. H. Leuba, G. H. Leno, J. Zlatanova, B. G. de Grooth, and J. Greve, “Unfolding individual nucleosomes by stretching single chromatin fibers with optical tweezers,” *Nat. Struct. Biol.* **8**, 606–610 (2001).
- G. Sinclair, P. Jordan, J. Courtial, M. Padgett, J. Cooper, and Z. J. Laczik, “Assembly of 3-dimensional structures using programmable holographic optical tweezers,” *Opt. Express* **12**, 5475–5480 (2004).
- S. C. Chapin, V. Germain, and E. R. Dufresne, “Automated trapping, assembly, and sorting with holographic optical tweezers,” *Opt. Express* **14**, 13095–13100 (2006).

- ⁸A. Barroso, T. Buscher, K. Ahlers, A. Studer, and C. Denz, "Optomechanically assisted assembly of surface-functionalized zeolite-l-based hybrid soft matter," *Part. Part. Syst. Charact.* **35**, 1800041 (2018).
- ⁹M. Woerdemann, S. Gläsener, F. Hörner, A. Devaux, L. D. Cola, and C. Denz, "Dynamic and reversible organization of zeolite l crystals induced by holographic optical tweezers," *Adv. Mater.* **22**, 4176–4179 (2010).
- ¹⁰H. Rubinsztajn-Dunlop, A. Forbes, M. V. Berry, M. R. Dennis, D. L. Andrews, M. Mansuripur, C. Denz, C. Alpmann, P. Banzer, T. Bauer, E. Karimi, L. Marrucci, M. Padgett, M. Ritsch-Marte, N. M. Litchinitser, N. P. Bigelow, C. Rosales-Guzmán, A. Belmonte, J. P. Torres, T. W. Neely, M. Baker, R. Gordon, A. B. Stilgoe, J. Romero, A. G. White, R. Fickler, A. E. Willner, G. Xie, B. McMorran, and A. M. Weiner, "Roadmap on structured light," *J. Opt.* **19**, 013001 (2017).
- ¹¹P. A. Santi, "Light sheet fluorescence microscopy: A review," *J. Histochem. Cytochem.* **59**, 129–138 (2011).
- ¹²A. H. Voie, D. Burns, and F. Spelman, "Orthogonal-plane fluorescence optical sectioning: Three-dimensional imaging of macroscopic biological specimens," *J. Microsc.* **170**, 229–236 (1993).
- ¹³S. W. Hell and J. Wichmann, "Breaking the diffraction resolution limit by stimulated emission: Stimulated-emission-depletion fluorescence microscopy," *Opt. Lett.* **19**, 780–782 (1994).
- ¹⁴A. Mair, A. Vaziri, G. Weihs, and A. Zeilinger, "Entanglement of the orbital angular momentum states of photons," *Nature* **412**, 313 (2001).
- ¹⁵M. Mirhosseini, O. S. Magaña-Loaiza, M. N. O'Sullivan, B. Rodenburg, M. Malik, M. P. Lavery, M. J. Padgett, D. J. Gauthier, and R. W. Boyd, "High-dimensional quantum cryptography with twisted light," *New J. Phys.* **17**, 033033 (2015).
- ¹⁶G. Gibson, J. Courtial, M. Padgett, M. Vasnetsov, V. Pas'ko, S. Barnett, and S. Franke-Arnold, "Free-space information transfer using light beams carrying orbital angular momentum," *Opt. Express* **12**, 5448–5456 (2004).
- ¹⁷G. Milione, M. P. J. Lavery, H. Huang, Y. Ren, G. Xie, T. A. Nguyen, E. Karimi, L. Marrucci, D. A. Nolan, R. R. Alfano, and A. E. Willner, "4 × 20 Gbit/s mode division multiplexing over free space using vector modes and a q-plate mode (de)multiplexer," *Opt. Lett.* **40**, 1980–1983 (2015).
- ¹⁸E. Otte, I. Nape, C. Rosales-Guzmán, C. Denz, A. Forbes, and B. Ndagano, "High-dimensional cryptography with spatial modes of light: Tutorial," *J. Opt. Soc. Am. B* **37**, A309–A323 (2020).
- ¹⁹B. Ndagano, B. Perez-Garcia, F. S. Roux, M. McLaren, C. Rosales-Guzman, Y. Zhang, O. Mouane, R. I. Hernandez-Aranda, T. Konrad, and A. Forbes, "Characterizing quantum channels with non-separable states of classical light," *Nat. Phys.* **13**, 397–402 (2017).
- ²⁰B. Ndagano, I. Nape, B. Perez-Garcia, S. Scholes, R. I. Hernandez-Aranda, T. Konrad, M. P. Lavery, and A. Forbes, "A deterministic detector for vector vortex states," *Sci. Rep.* **7**, 13882 (2017).
- ²¹E. R. Dufresne and a. G. Grier, "Optical tweezer arrays and optical substrates created with diffractive optics," *Rev. Sci. Instrum.* **69**, 1974–1977 (1998).
- ²²J. Liesener, M. Reicherter, T. Haist, and H. J. Tiziani, "Multi-functional optical tweezers using computer-generated holograms," *Opt. Commun.* **185**, 77–82 (2000).
- ²³E. R. Dufresne, G. C. Spalding, M. T. Dearing, S. A. Sheets, and D. G. Grier, "Computer-generated holographic optical tweezer arrays," *Rev. Sci. Instrum.* **72**, 1810–1816 (2001).
- ²⁴J. A. Davis, D. M. Cottrell, J. Campos, M. J. Yzuel, and I. Moreno, "Encoding amplitude information onto phase-only filters," *Appl. Opt.* **38**, 5004–5013 (1999).
- ²⁵C. Rosales-Guzmán and A. Forbes, *How to Shape Light with Spatial Light Modulators* (SPIE Press, 2017).
- ²⁶M. J. O'Brien and D. G. Grier, "Above and beyond: Holographic tracking of axial displacements in holographic optical tweezers," *Opt. Express* **27**, 25375–25383 (2019).
- ²⁷B. Kemper, Á. Barroso, M. Woerdemann, L. Dewenter, A. Vollmer, R. Schubert, A. Mellmann, G. von Bally, and C. Denz, "Towards 3D modelling and imaging of infection scenarios at the single cell level using holographic optical tweezers and digital holographic microscopy," *J. Biophotonics* **6**, 260–266 (2013).
- ²⁸U. G. Bütaite, G. M. Gibson, Y.-L. D. Ho, M. Taverne, J. M. Taylor, and D. B. Phillips, "Indirect optical trapping using light driven micro-rotors for reconfigurable hydrodynamic manipulation," *Nat. Commun.* **10**, 1215 (2019).
- ²⁹D. Palima and J. Glückstad, "Gearing up for optical microrobotics: Micromanipulation and actuation of synthetic microstructures by optical forces," *Laser Photonics Rev.* **7**, 478–494 (2013).
- ³⁰Á. Barroso, S. Landwerth, M. Woerdemann, C. Alpmann, T. Buscher, M. Becker, A. Studer, and C. Denz, "Optical assembly of bio-hybrid micro-robots," *Biomed. Microdevices* **17**, 26 (2015).
- ³¹S. Sato, M. Ishigure, and H. Inaba, "Optical trapping and rotational manipulation of microscopic particles and biological cells using higher-order mode Nd:YAG laser beams," *Electron. Lett.* **27**, 1831–1832 (1991).
- ³²A. Jesacher, S. Fühapter, S. Bernet, and M. Ritsch-Marte, "Size selective trapping with optical 'cogwheel' tweezers," *Opt. Express* **12**, 4129–4135 (2004).
- ³³C. Alpmann, C. Schöler, and C. Denz, "Elegant Gaussian beams for enhanced optical manipulation," *Appl. Phys. Lett.* **106**, 241102 (2015).
- ³⁴V. Garcés-Chávez, D. McGloin, H. Melville, W. Sibbett, and K. Dholakia, "Simultaneous micromanipulation in multiple planes using a self-reconstructing light beam," *Nature* **419**, 145 (2002).
- ³⁵C. Alpmann, R. Bowman, M. Woerdemann, M. Padgett, and C. Denz, "Mathieu beams as versatile light moulds for 3D micro particle assemblies," *Opt. Express* **18**, 26084–26091 (2010).
- ³⁶D. B. Ruffner and D. G. Grier, "Optical conveyors: A class of active tractor beams," *Phys. Rev. Lett.* **109**, 163903 (2012).
- ³⁷J. Baumgartl, M. Mazilu, and K. Dholakia, "Optically mediated particle clearing using airy wavepackets," *Nat. Photonics* **2**, 675 (2008).
- ³⁸Y. Roichman and D. G. Grier, *Opt. Lett.* **31**, 1675 (2006).
- ³⁹S.-H. Lee, Y. Roichman, and D. G. Grier, "Optical solenoid beams," *Opt. Express* **18**, 6988–6993 (2010).
- ⁴⁰E. R. Shanblatt and D. G. Grier, "Extended and knotted optical traps in three dimensions," *Opt. Express* **19**, 5833–5838 (2011).
- ⁴¹L. Allen, S. M. Barnett, and M. J. Padgett, *Optical Angular Momentum* (CRC Press, 2003).
- ⁴²H. He, M. E. J. Friese, N. R. Heckenberg, and H. Rubinsztajn-Dunlop, "Direct observation of transfer of angular momentum to absorptive particles from a laser beam with a phase singularity," *Phys. Rev. Lett.* **75**, 826–829 (1995).
- ⁴³M. Friese, J. Enger, H. Rubinsztajn-Dunlop, and N. Heckenberg, "Optical angular-momentum transfer to trapped absorbing particles," *Phys. Rev. A* **54**, 1593–1596 (1996).
- ⁴⁴N. Simpson, K. Dholakia, L. Allen, and M. Padgett, "Mechanical equivalence of spin and orbital angular momentum of light: An optical spanner," *Opt. Lett.* **22**, 52–54 (1997).
- ⁴⁵M. Padgett and R. Bowman, "Tweezers with a twist," *Nat. Photonics* **5**, 343–348 (2011).
- ⁴⁶A. Belmonte, C. Rosales-Guzmán, and J. P. Torres, "Measurement of flow vorticity with helical beams of light," *Optica* **2**, 1002–1005 (2015).
- ⁴⁷C. Rosales-Guzmán, K. Volke-Sepulveda, and J. P. Torres, "Light with enhanced optical chirality," *Opt. Lett.* **37**, 3486–3488 (2012).
- ⁴⁸M. Friese, T. Nieminen, N. Heckenberg, and H. Rubinsztajn-Dunlop, "Optical alignment and spinning of laser-trapped microscopic particles," *Nature* **394**, 348–350 (1998).
- ⁴⁹A. Bekshaev, K. Y. Bliokh, and M. Soskin, "Internal flows and energy circulation in light beams," *J. Opt.* **13**, 053001 (2011).
- ⁵⁰E. Otte, E. Asché, and C. Denz, "Shaping optical spin flow topologies by the translation of tailored orbital phase flow," *J. Opt.* **21**, 064001 (2019).
- ⁵¹E. Otte, C. Schlickriede, C. Alpmann, and C. Denz, "Complex light fields enter a new dimension: Holographic modulation of polarization in addition to amplitude and phase," *Proc. SPIE* **9379**, 937908 (2015).
- ⁵²C. Alpmann, C. Schlickriede, E. Otte, and C. Denz, "Dynamic modulation of Poincaré beams," *Sci. Rep.* **7**, 8076 (2017).
- ⁵³E. Otte, C. Rosales-Guzmán, B. Ndagano, C. Denz, and A. Forbes, "Entanglement beating in free space through spin-orbit coupling," *Light: Sci. Appl.* **7**, 18009 (2018).
- ⁵⁴C. J. Gibson, P. Bevington, G.-L. Oppo, and A. M. Yao, "Control of polarization rotation in nonlinear propagation of fully structured light," *Phys. Rev. A* **97**, 033832 (2018).
- ⁵⁵E. Otte, K. Tekce, and C. Denz, "Spatial multiplexing for tailored fully-structured light," *J. Opt.* **20**, 105606 (2018).
- ⁵⁶R. Dorn, S. Quabis, and G. Leuchs, "Sharper focus for a radially polarized light beam," *Phys. Rev. Lett.* **91**, 233901 (2003).

- ⁵⁷S. Quabis, R. Dorn, M. Eberler, O. Glöckl, and G. Leuchs, "Focusing light to a tighter spot," *Opt. Commun.* **179**, 1–7 (2000).
- ⁵⁸N. Bhebbhe, P. A. Williams, C. Rosales-Guzmán, V. Rodríguez-Fajardo, and A. Forbes, "A vector holographic optical trap," *Sci. Rep.* **8**, 17387 (2018).
- ⁵⁹T. A. Nieminen, N. R. Heckenberg, and H. Rubinsztein-Dunlop, "Forces in optical tweezers with radially and azimuthally polarized trapping beams," *Opt. Lett.* **33**, 122–124 (2008).
- ⁶⁰S. Skelton, M. Sergides, R. Saija, M. Iatì, O. Maragó, and P. Jones, "Trapping volume control in optical tweezers using cylindrical vector beams," *Opt. Lett.* **38**, 28–30 (2013).
- ⁶¹W. Chen and Q. Zhan, "Three-dimensional focus shaping with cylindrical vector beams," *Opt. Commun.* **265**, 411–417 (2006).
- ⁶²E. Otte, K. Tekce, and C. Denz, "Tailored intensity landscapes by tight focusing of singular vector beams," *Opt. Express* **25**, 20194–20201 (2017).
- ⁶³X. Jiao, S. Liu, Q. Wang, X. Gan, P. Li, and J. Zhao, "Redistributing energy flow and polarization of a focused azimuthally polarized beam with rotationally symmetric sector-shaped obstacles," *Opt. Lett.* **37**, 1041–1043 (2012).
- ⁶⁴I. Freund, "Cones, spirals, and Möbius strips, elliptically polarized light," *Opt. Commun.* **249**, 7–22 (2005).
- ⁶⁵T. Bauer, P. Banzer, E. Karimi, S. Orlov, A. Rubano, L. Marrucci, E. Santamato, R. W. Boyd, and G. Leuchs, "Observation of optical polarization Möbius strips," *Science* **347**, 964–966 (2015).
- ⁶⁶K. Tekce, E. Otte, and C. Denz, "Optical singularities and Möbius strip arrays in tailored non-paraxial light fields," *Opt. Express* **27**, 29685–29696 (2019).
- ⁶⁷P. Lebedev, "The experimental study of the pressure of the light," *Ann. Phys.* **6**, 433 (1901).
- ⁶⁸J. Maxwell, *A Treatise on Electricity and Magnetism* (Clarendon Press, Oxford, 1873), Vol. 2.
- ⁶⁹E. F. Nichols and G. F. Hull, "A preliminary communication on the pressure of heat and light radiation," *Phys. Rev. Ser. I* **13**, 307 (1901).
- ⁷⁰E. F. Nichols and G. F. Hull, "The pressure due to radiation. (Second paper)," *Phys. Rev. Ser. I* **17**, 26 (1903).
- ⁷¹Y. Harada and T. Asakura, "Radiation forces on a dielectric sphere in the Rayleigh scattering regime," *Opt. Commun.* **124**, 529 (1996).
- ⁷²K. Svoboda and S. M. Block, "Biological applications of optical forces," *Annu. Rev. Biophys. Biomol. Struct.* **23**, 247–285 (1994).
- ⁷³D. J. Stevenson, F. J. Gunn-Moore, and K. Dholakia, "Light forces the pace: Optical manipulation for biophotonics," *J. Biomed. Opt.* **15**, 041503 (2010).
- ⁷⁴W. W. Sugden, R. Meissner, T. Aegerter-Wilmsen, R. Tsaryk, E. V. Leonard, J. Bussmann, M. J. Hamm, W. Herzog, Y. Jin, L. Jakobsson *et al.*, "Endoglin controls blood vessel diameter through endothelial cell shape changes in response to haemodynamic cues," *Nat. Cell Biol.* **19**, 653 (2017).
- ⁷⁵K. C. Neuman and S. M. Block, "Optical trapping," *Rev. Sci. Instrum.* **75**, 2787–2809 (2004).
- ⁷⁶K. Berg-Sørensen and H. Flyvbjerg, "Power spectrum analysis for optical tweezers," *Rev. Sci. Instrum.* **75**, 594–612 (2004).
- ⁷⁷E.-L. Florin, A. Pralle, E. Stelzer, and J. Hörber, "Photonic force microscope calibration by thermal noise analysis," *Appl. Phys. A: Mater. Sci. Process.* **66**, S75–S78 (1998).
- ⁷⁸L. P. Ghislain and W. W. Webb, "Scanning-force microscope based on an optical trap," *Opt. Lett.* **18**, 1678–1680 (1993).
- ⁷⁹M. Jahnel, M. Behrndt, A. Jannasch, E. Schäffer, and S. W. Grill, "Measuring the complete force field of an optical trap," *Opt. Lett.* **36**, 1260–1262 (2011).
- ⁸⁰F. M. Fazal and S. M. Block, "Optical tweezers study life under tension," *Nat. Photonics* **5**, 318 (2011).
- ⁸¹M. Villangca, D. Casey, and J. Glückstad, "Optically-controlled platforms for transfection and single-and sub-cellular surgery," *Biophys. Rev.* **7**, 379–390 (2015).
- ⁸²P. Rodríguez-Sevilla, L. Labrador-Páez, D. Jaque, and P. Haro-González, "Optical trapping for biosensing: Materials and applications," *J. Mater. Chem. B* **5**, 9085–9101 (2017).
- ⁸³A.-I. Bunea and J. Glückstad, "Strategies for optical trapping in biological samples: Aiming at microrobotic surgeons," *Laser Photonics Rev.* **13**, 1800227 (2019).
- ⁸⁴D. G. Grier, "Optical tweezers in colloid and interface science," *Curr. Opin. Colloid Interface Sci.* **2**, 264–270 (1997).
- ⁸⁵M. P. MacDonald, G. C. Spalding, and K. Dholakia, "Microfluidic sorting in an optical lattice," *Nature* **426**, 421 (2003).
- ⁸⁶I. Perch-Nielsen, D. Palima, J. S. Dam, and J. Glückstad, "Parallel particle identification and separation for active optical sorting," *J. Opt. A: Pure Appl. Opt.* **11**, 034013 (2009).
- ⁸⁷A. Jonáš and P. Zemanek, "Light at work: The use of optical forces for particle manipulation, sorting, and analysis," *Electrophoresis* **29**, 4813–4851 (2008).
- ⁸⁸J. Leach, H. Mushfique, R. di Leonardo, M. Padgett, and J. Cooper, "An optically driven pump for microfluidics," *Lab Chip* **6**, 735–739 (2006).
- ⁸⁹D. G. Grier, "A revolution in optical manipulation," *Nature* **424**, 810 (2003).
- ⁹⁰J. C. Crocker and D. G. Grier, "Microscopic measurement of the pair interaction potential of charge-stabilized colloid," *Phys. Rev. Lett.* **73**, 352 (1994).
- ⁹¹J. E. Curtis, B. A. Koss, and D. G. Grier, "Dynamic holographic optical tweezers," *Opt. Commun.* **207**, 169–175 (2002).
- ⁹²M. Polin, K. Ladavac, S.-H. Lee, Y. Roichman, and D. G. Grier, "Optimized holographic optical traps," *Opt. Express* **13**, 5831–5845 (2005).
- ⁹³C. Hesselberg, M. Woerdemann, A. Hermerschmidt, and C. Denz, "Controlling ghost traps in holographic optical tweezers," *Opt. Lett.* **36**, 3657–3659 (2011).
- ⁹⁴J. E. Curtis, C. H. Schmitz, and J. P. Spatz, "Symmetry dependence of holograms for optical trapping," *Opt. Lett.* **30**, 2086–2088 (2005).
- ⁹⁵M. Montes-Usategui, E. Pleguezuelos, J. Andilla, and E. Martín-Badosa, "Fast generation of holographic optical tweezers by random mask encoding of fourier components," *Opt. Express* **14**, 2101–2107 (2006).
- ⁹⁶J. Mas, M. S. Roth, E. Martín-Badosa, and M. Montes-Usategui, "Adding functionalities to precomputed holograms with random mask multiplexing in holographic optical tweezers," *Appl. Opt.* **50**, 1417–1424 (2011).
- ⁹⁷R. W. Gerchberg and W. O. Saxton, "Phase retrieval by iterated projections," *Optik* **35**, 237 (1972).
- ⁹⁸J. R. Fienup, "Phase retrieval algorithms: A comparison," *Appl. Opt.* **21**, 2758–2769 (1982).
- ⁹⁹M. Padgett and R. D. Leonardo, "Holographic optical tweezers and their relevance to lab on chip devices," *Lab Chip* **11**, 1196–1205 (2011).
- ¹⁰⁰E. Lasnoy, O. Wagner, E. Edri, and H. Shpalsman, "Drag controlled formation of polymeric colloids with optical traps," *Lab Chip* **19**, 3543–3551 (2019).
- ¹⁰¹L. Marrucci, C. Manzo, and D. Paparo, "Optical spin-to-orbital angular momentum conversion in inhomogeneous anisotropic media," *Phys. Rev. Lett.* **96**, 163905 (2006).
- ¹⁰²B. Piccirillo, V. D'Ambrosio, S. Slussarenko, L. Marrucci, and E. Santamato, "Photon spin-to-orbital angular momentum conversion via an electrically tunable q-plate," *Appl. Phys. Lett.* **97**, 241104 (2010).
- ¹⁰³B. Desiatov, N. Mazurski, Y. Fainman, and U. Levy, "Polarization selective beam shaping using nanoscale dielectric metasurfaces," *Opt. Express* **23**, 22611–22618 (2015).
- ¹⁰⁴S. Keren-Zur, O. Avayu, L. Michaeli, and T. Ellenbogen, "Nonlinear beam shaping with plasmonic metasurfaces," *ACS Photonics* **3**, 117–123 (2016).
- ¹⁰⁵O. Avayu, O. Eisenbach, R. Ditzovski, and T. Ellenbogen, "Optical metasurfaces for polarization-controlled beam shaping," *Opt. Lett.* **39**, 3892–3895 (2014).
- ¹⁰⁶D. Lin, P. Fan, E. Hasman, and M. L. Brongersma, "Dielectric gradient metasurface optical elements," *Science* **345**, 298–302 (2014).
- ¹⁰⁷W. T. Chen, M. Khorasaninejad, A. Y. Zhu, J. Oh, R. C. Devlin, A. Zaidi, and F. Capasso, "Generation of wavelength-independent subwavelength Bessel beams using metasurfaces," *Light: Sci. Appl.* **6**, e16259–e16259 (2017).
- ¹⁰⁸P. Genevet, F. Capasso, F. Aieta, M. Khorasaninejad, and R. Devlin, "Recent advances in planar optics: From plasmonic to dielectric metasurfaces," *Optica* **4**, 139–152 (2017).
- ¹⁰⁹V.-C. Su, C. H. Chu, G. Sun, and D. P. Tsai, "Advances in optical metasurfaces: Fabrication and applications," *Opt. Express* **26**, 13148–13182 (2018).
- ¹¹⁰A. M. Shaltout, V. M. Shalaev, and M. L. Brongersma, "Spatiotemporal light control with active metasurfaces," *Science* **364**, eaat3100 (2019).
- ¹¹¹H. Kogelnik and T. Li, "Laser beams and resonators," *Appl. Opt.* **5**, 1550–1567 (1966).
- ¹¹²A. Siegman, *Lasers* (University Science Books, 1986).
- ¹¹³M. A. Bandres and J. C. Gutiérrez-Vega, "Ince Gaussian beams," *Opt. Lett.* **29**, 144–146 (2004).

- ¹¹⁴M. Woerdemann, C. Alpmann, and C. Denz, "Optical assembly of microparticles into highly ordered structures using Ince-Gaussian beams," *Appl. Phys. Lett.* **98**, 111101 (2011).
- ¹¹⁵S. Mohanty, K. Mohanty, and M. Berns, "Organization of microscale objects using a microfabricated optical fiber," *Opt. Lett.* **33**, 2155–2157 (2008).
- ¹¹⁶A. Siegman, "Hermite–Gaussian functions of complex argument as optical-beam eigenfunctions," *J. Opt. Soc. Am.* **63**, 1093–1094 (1973).
- ¹¹⁷M. Bandres, "Elegant Ince-Gaussian beams," *Opt. Lett.* **29**, 1724–1726 (2004).
- ¹¹⁸J. Durnin, J. J. Miceli, and J. H. Eberly, "Diffraction-free beams," *Phys. Rev. Lett.* **58**, 1499–1501 (1987).
- ¹¹⁹Z. Bouchal, J. Wagner, and M. Chlup, "Self-reconstruction of a distorted non-diffracting beam," *Opt. Commun.* **151**, 207–211 (1998).
- ¹²⁰F. Gori, G. Guattari, and C. Padovani, "Bessel-Gauss beams," *Opt. Commun.* **64**, 491–495 (1987).
- ¹²¹J. C. Gutiérrez-Vega and M. A. Bandres, "Helmholtz–gauss waves," *J. Opt. Soc. Am. A* **22**, 289–298 (2005).
- ¹²²M. Boguslawski, P. Rose, and C. Denz, "Increasing the structural variety of discrete nondiffracting wave fields," *Phys. Rev. A* **84**, 013832 (2011).
- ¹²³K. Dholakia and W. Lee, "Optical trapping takes shape: The use of structured light fields," *Adv. At., Mol., Opt. Phys.* **56**, 261–337 (2008).
- ¹²⁴J. Chen, J. Ng, Z. Lin, and C. Chan, "Optical pulling force," *Nat. Photonics* **5**, 531 (2011).
- ¹²⁵X. Li, J. Chen, Z. Lin, and J. Ng, "Optical pulling at macroscopic distances," *Sci. Adv.* **5**, eaau7814 (2019).
- ¹²⁶W. Ding, T. Zhu, L.-M. Zhou, and C.-W. Qiu, "Photonic tractor beams: A review," *Adv. Photonics* **1**, 1 (2019).
- ¹²⁷M. R. Dennis, K. O'Holleran, and M. J. Padgett, "Singular optics: Optical vortices and polarization singularities," in *Progress in Optics*, edited by E. Wolf (Elsevier, 2009), Vol. 53, pp. 293–363.
- ¹²⁸M. Berry and C. Upstill, "Catastrophe optics: Morphologies of caustics and their diffraction patterns," *Prog. Opt.* **18**, 257–346 (1980).
- ¹²⁹J. F. Nye, *Natural Focusing and Fine Structure of Light: Caustics and Wave Dislocations* (CRC Press, 1999).
- ¹³⁰V. I. Arnol'd, *Catastrophe Theory* (Springer Science & Business Media, 2003).
- ¹³¹T. Poston and I. Stewart, *Catastrophe Theory and Its Applications* (Dover Publications Inc., New York, 1996).
- ¹³²M. V. Berry and N. L. Balazs, "Nonspreading wave packets," *Am. J. Phys.* **47**, 264–267 (1979).
- ¹³³G. A. Siviloglou and D. N. Christodoulides, "Accelerating finite energy airy beams," *Opt. Lett.* **32**, 979–981 (2007).
- ¹³⁴G. Siviloglou, J. Broky, A. Dogariu, and D. Christodoulides, "Observation of accelerating airy beams," *Phys. Rev. Lett.* **99**, 213901 (2007).
- ¹³⁵J. D. Ring, J. Lindberg, A. Mourka, M. Mazilu, K. Dholakia, and M. R. Dennis, "Auto-focusing and self-healing of Pearcey beams," *Opt. Express* **20**, 18955–18966 (2012).
- ¹³⁶A. Zannotti, F. Diebel, and C. Denz, "Dynamics of the optical swallowtail catastrophe," *Optica* **4**, 1157–1162 (2017).
- ¹³⁷A. Zannotti, F. Diebel, M. Boguslawski, and C. Denz, "Optical catastrophes of the swallowtail and butterfly beams," *New J. Phys.* **19**, 053004 (2017).
- ¹³⁸A. Zannotti, M. Rüschbaum, and C. Denz, "Pearcey solitons in curved non-linear photonic caustic lattices," *J. Opt.* **19**, 094001 (2017).
- ¹³⁹A. Y. Bekshaev and M. Soskin, "Transverse energy flows in vectorial fields of paraxial beams with singularities," *Opt. Commun.* **271**, 332–348 (2007).
- ¹⁴⁰F. J. Belinfante, "On the current and the density of the electric charge, the energy, the linear momentum and the angular momentum of arbitrary fields," *Physica* **7**, 449–474 (1940).
- ¹⁴¹K. Y. Bliokh, A. Y. Bekshaev, and F. Nori, "Dual electromagnetism: Helicity, spin, momentum and angular momentum," *New J. Phys.* **15**, 033026 (2013).
- ¹⁴²K. Mita, "Virtual probability current associated with the spin," *Am. J. Phys.* **68**, 259–264 (2000).
- ¹⁴³A. Y. Bekshaev, K. Y. Bliokh, and F. Nori, "Transverse spin and momentum in two-wave interference," *Phys. Rev. X* **5**, 011039 (2015).
- ¹⁴⁴M. Neugebauer, T. Bauer, A. Aiello, and P. Banzer, "Measuring the transverse spin density of light," *Phys. Rev. Lett.* **114**, 063901 (2015).
- ¹⁴⁵M. Antognozzi, C. Bermingham, R. Harniman, S. Simpson, J. Senior, R. Hayward, H. Hoerber, M. Dennis, A. Bekshaev, K. Bliokh *et al.*, "Direct measurements of the extraordinary optical momentum and transverse spin-dependent force using a nano-cantilever," *Nat. Phys.* **12**, 731–735 (2016).
- ¹⁴⁶V. Svak, O. Brzobohatý, M. Šiler, P. Ják, J. Kaňka, P. Zemánek, and S. Simpson, "Transverse spin forces and non-equilibrium particle dynamics in a circularly polarized vacuum optical trap," *Nat. Commun.* **9**, 5453 (2018).
- ¹⁴⁷K. Y. Bliokh, A. Y. Bekshaev, and F. Nori, "Extraordinary momentum and spin in evanescent waves," *Nat. Commun.* **5**, 3300 (2014).
- ¹⁴⁸I. Freund, A. I. Mokhun, M. S. Soskin, O. V. Angelsky, and I. I. Mokhun, "Stokes singularity relations," *Opt. Lett.* **27**, 545–547 (2002).
- ¹⁴⁹J. B. Götte and S. M. Barnett, *Light Beams Carrying Orbital Angular Momentum* (Cambridge University Press, 2012), Chap. 1, pp. 1–30.
- ¹⁵⁰G. Tkachenko and E. Brasselet, "Optofluidic sorting of material chirality by chiral light," *Nat. Commun.* **5**, 3577 (2014).
- ¹⁵¹H. Chen, W. Lu, X. Yu, C. Xue, S. Liu, and Z. Lin, "Optical torque on small chiral particles in generic optical fields," *Opt. Express* **25**, 32867–32878 (2017).
- ¹⁵²L. Allen, M. Beijersbergen, R. Spreeuw, and J. Woerdman, "Orbital angular-momentum of light and the transformation of Laguerre-Gaussian laser modes," *Phys. Rev. A* **45**, 8185–8189 (1992).
- ¹⁵³S. Van Enk and G. Nienhuis, "Eigenfunction description laser beams orbital angular momentum light," *Opt. Commun.* **94**, 147–158 (1992).
- ¹⁵⁴M. S. Soskin and M. V. Vasnetsov, "Singular optics," *Prog. Opt.* **42**, 219–277 (2001).
- ¹⁵⁵Y. Shen, X. Wang, Z. Xie, C. Min, X. Fu, Q. Liu, M. Gong, and X. Yuan, "Optical vortices 30 years on: OAM manipulation from topological charge to multiple singularities," *Light: Sci. Appl.* **8**, 1–29 (2019).
- ¹⁵⁶J. A. Rodrigo and T. Alieva, "Polymorphic beams and nature inspired circuits for optical current," *Sci. Rep.* **6**, 35341 (2016).
- ¹⁵⁷K. Volke-Sepulveda, V. Garcés-Chávez, S. Chávez-Cerda, J. Arlt, and K. Dholakia, "Orbital angular momentum of a high-order Bessel light beam," *J. Opt. B: Quantum Semiclassical Opt.* **4**, S82 (2002).
- ¹⁵⁸M. Chen, S. Huang, X. Liu, Y. Chen, and W. Shao, "Optical trapping and rotating of micro-particles using the circular airy vortex beams," *Appl. Phys. B* **125**, 184 (2019).
- ¹⁵⁹M. Bandres and J. Gutierrez-Vega, "Ince-Gaussian modes of the paraxial wave equation and stable resonators," *J. Opt. Soc. Am. A* **21**, 873–880 (2004).
- ¹⁶⁰R. A. Terborg and K. Volke-Sepulveda, "Quantitative characterization of the energy circulation in helical beams by means of near-field diffraction," *Opt. Express* **21**, 3379–3387 (2013).
- ¹⁶¹W. N. Plick, M. Krenn, R. Fickler, S. Ramelow, and A. Zeilinger, "Quantum orbital angular momentum of elliptically symmetric light," *Phys. Rev. A* **87**, 033806 (2013).
- ¹⁶²A. Zannotti, J. M. Vasiljević, D. V. Timotijević, D. M. Jović Savić, and C. Denz, "Visualizing the energy flow of tailored light," *Adv. Opt. Mater.* **6**, 1701355 (2018).
- ¹⁶³Y. Roichman and D. G. Grier, "Three-dimensional holographic ring traps," *Proc. SPIE* **6483**, 64830F (2007).
- ¹⁶⁴Y. Roichman, D. G. Grier, and G. Zaslavsky, "Anomalous collective dynamics in optically driven colloidal rings," *Phys. Rev. E* **75**, 020401 (2007).
- ¹⁶⁵A. S. Ostrovsky, C. Rickenstorff-Parrao, and V. Arrizón, "Generation of the 'perfect' optical vortex using a liquid-crystal spatial light modulator," *Opt. Lett.* **38**, 534–536 (2013).
- ¹⁶⁶M. Chen, M. Mazilu, Y. Arita, E. M. Wright, and K. Dholakia, "Dynamics of microparticles trapped in a perfect vortex beam," *Opt. Lett.* **38**, 4919–4922 (2013).
- ¹⁶⁷J. Leach, E. Yao, and M. J. Padgett, "Observation of the vortex structure of a non-integer vortex beam," *New J. Phys.* **6**, 71 (2004).
- ¹⁶⁸G. Tkachenko, M. Chen, K. Dholakia, and M. Mazilu, "Is it possible to create a perfect fractional vortex beam?," *Optica* **4**, 330–333 (2017).
- ¹⁶⁹Y. Liang, M. Lei, S. Yan, M. Li, Y. Cai, Z. Wang, X. Yu, and B. Yao, "Rotating of low-refractive-index microparticles with a quasi-perfect optical vortex," *Appl. Opt.* **57**, 79–84 (2018).
- ¹⁷⁰J. A. Rodrigo, T. Alieva, E. Abramochkin, and I. Castro, "Shaping of light beams along curves in three dimensions," *Opt. Express* **21**, 20544–20555 (2013).
- ¹⁷¹J. A. Rodrigo, M. Angulo, and T. Alieva, "Dynamic morphing of 3D curved laser traps for all-optical manipulation of particles," *Opt. Express* **26**, 18608–18620 (2018).

- ¹⁷²A. Belmonte and J. P. Torres, "Optical doppler shift with structured light," *Opt. Lett.* **36**, 4437–4439 (2011).
- ¹⁷³C. Rosales-Guzmán, N. Hermosa, A. Belmonte, and J. P. Torres, "Experimental detection of transverse particle movement with structured light," *Sci. Rep.* **3**, 2815 (2013).
- ¹⁷⁴M. Veiga-Gutiérrez, M. Woerdemann, E. Prasetyanto, C. Denz, and L. De Cola, "Optical-tweezers assembly-line for the construction of complex functional zeolite I structures," *Adv. Mater.* **24**, 5199–5204 (2012).
- ¹⁷⁵I. Freund, "Polarization singularity indices in Gaussian laser beams," *Opt. Commun.* **201**, 251–270 (2002).
- ¹⁷⁶Q. Zhan, "Cylindrical vector beams: From mathematical concepts to applications," *Adv. Opt. Photonics* **1**, 1–57 (2009).
- ¹⁷⁷A. Dudley, Y. Li, T. Mhlanga, M. Escuti, and A. Forbes, "Generating and measuring nondiffracting vector Bessel beams," *Opt. Lett.* **38**, 3429–3432 (2013).
- ¹⁷⁸G. Milione, A. Dudley, T. A. Nguyen, O. Chakraborty, E. Karimi, A. Forbes, and R. R. Alfano, "Measuring the self-healing of the spatially inhomogeneous states of polarization of vector Bessel beams," *J. Opt.* **17**, 035617 (2015).
- ¹⁷⁹E. Otte, I. Nape, C. Rosales-Guzmán, A. Vallés, C. Denz, and A. Forbes, "Recovery of nonseparability in self-healing vector Bessel beams," *Phys. Rev. A* **98**, 053818 (2018).
- ¹⁸⁰A. M. Beckley, T. G. Brown, and M. A. Alonso, "Full Poincaré beams," *Opt. Express* **18**, 10777–10785 (2010).
- ¹⁸¹E. Otte and C. Denz, "Sculpting complex polarization singularity networks," *Opt. Lett.* **43**, 5821–5824 (2018).
- ¹⁸²H. Garcia-Gracia and J. C. Gutiérrez-Vega, "Polarization singularities in non-diffracting Mathieu–Poincaré beams," *J. Opt.* **18**, 014006 (2016).
- ¹⁸³E. J. Galvez, S. Khadka, W. H. Schubert, and S. Nomoto, "Poincaré-beam patterns produced by nonseparable superpositions of Laguerre–Gauss and polarization modes of light," *Appl. Opt.* **51**, 2925–2934 (2012).
- ¹⁸⁴C. Maurer, A. Jesacher, S. Fürhapter, S. Bernet, and M. Ritsch-Marte, "Tailoring of arbitrary optical vector beams," *New J. Phys.* **9**, 78 (2007).
- ¹⁸⁵Z.-Y. Rong, Y.-J. Han, S.-Z. Wang, and C.-S. Guo, "Generation of arbitrary vector beams with cascaded liquid crystal spatial light modulators," *Opt. Express* **22**, 1636–1644 (2014).
- ¹⁸⁶Z. Chen, T. Zeng, B. Qian, and J. Ding, "Complete shaping of optical vector beams," *Opt. Express* **23**, 17701–17710 (2015).
- ¹⁸⁷C. Rosales-Guzmán, N. Bhebhe, and A. Forbes, "Simultaneous generation of multiple vector beams on a single SLM," *Opt. Express* **25**, 25697–25706 (2017).
- ¹⁸⁸Y.-Y. Xie, Z.-J. Cheng, X. Liu, B.-Y. Wang, Q.-Y. Yue, and C.-S. Guo, "Simple method for generation of vector beams using a small-angle birefringent beam splitter," *Opt. Lett.* **40**, 5109–5112 (2015).
- ¹⁸⁹Y. Liu, X. Ling, X. Yi, X. Zhou, H. Luo, and S. Wen, "Realization of polarization evolution on higher-order Poincaré sphere with metasurface," *Appl. Phys. Lett.* **104**, 191110 (2014).
- ¹⁹⁰S.-M. Li, S.-X. Qian, L.-J. Kong, Z.-C. Ren, Y. Li, C. Tu, and H.-T. Wang, "An efficient and robust scheme for controlling the states of polarization in a Sagnac interferometric configuration," *Europhys. Lett.* **105**, 64006 (2014).
- ¹⁹¹R. Liu, L.-J. Kong, W.-R. Qi, S.-Y. Huang, Z.-X. Wang, C. Tu, Y. Li, and H.-T. Wang, "Compact, robust, and high-efficiency generator of vector optical fields," *Opt. Lett.* **44**, 2382–2385 (2019).
- ¹⁹²S. Chen, X. Zhou, Y. Liu, X. Ling, H. Luo, and S. Wen, "Generation of arbitrary cylindrical vector beams on the higher order Poincaré sphere," *Opt. Lett.* **39**, 5274–5276 (2014).
- ¹⁹³J. Mendoza-Hernández, M. F. Ferrer-García, J. A. Rojas-Santana, and D. Lopez-Mago, "Cylindrical vector beam generator using a two-element interferometer," *Opt. Express* **27**, 31810–31819 (2019).
- ¹⁹⁴V. Kumar and N. K. Viswanathan, "Topological structures in the Poynting vector field: An experimental realization," *Opt. Lett.* **38**, 3886–3889 (2013).
- ¹⁹⁵V. Kumar and N. K. Viswanathan, "Topological structures in vector-vortex beam fields," *J. Opt. Soc. Am. B* **31**, A40–A45 (2014).
- ¹⁹⁶F. Cardano, E. Karimi, L. Marrucci, C. de Lisio, and E. Santamato, "Generation and dynamics of optical beams with polarization singularities," *Opt. Express* **21**, 8815–8820 (2013).
- ¹⁹⁷I. Nape, E. Otte, A. Vallés, C. Rosales-Guzmán, F. Cardano, C. Denz, and A. Forbes, "Self-healing high-dimensional quantum key distribution using hybrid spin-orbit Bessel states," *Opt. Express* **26**, 26946–26960 (2018).
- ¹⁹⁸X. Yi, X. Ling, Z. Zhang, Y. Li, X. Zhou, Y. Liu, S. Chen, H. Luo, and S. Wen, "Generation of cylindrical vector vortex beams by two cascaded metasurfaces," *Opt. Express* **22**, 17207–17215 (2014).
- ¹⁹⁹D. Naidoo, F. S. Roux, A. Dudley, I. Litvin, B. Piccirillo, L. Marrucci, and A. Forbes, "Controlled generation of higher-order Poincaré sphere beams from a laser," *Nat. Photonics* **10**, 327 (2016).
- ²⁰⁰C. He, J. Chang, Q. Hu, J. Wang, J. Antonello, H. He, S. Liu, J. Lin, B. Dai, D. S. Elson *et al.*, "Complex vectorial optics through gradient index lens cascades," *Nat. Commun.* **10**, 4264 (2019).
- ²⁰¹W. Han, Y. Yang, W. Cheng, and Q. Zhan, "Vectorial optical field generator for the creation of arbitrarily complex fields," *Opt. Express* **21**, 20692–20706 (2013).
- ²⁰²E. Otte, C. Alpmann, and C. Denz, "Higher-order polarization singularities in tailored vector beams," *J. Opt.* **18**, 074012 (2016).
- ²⁰³I. Freund, "Polarization flowers," *Opt. Commun.* **199**, 47–63 (2001).
- ²⁰⁴B. Schaefer, E. Collett, R. Smyth, D. Barrett, and B. Fraher, "Measuring the Stokes polarization parameters," *Am. J. Phys.* **75**, 163–168 (2007).
- ²⁰⁵S. Liu, S. Qi, Y. Zhang, P. Li, D. Wu, L. Han, and J. Zhao, "Highly efficient generation of arbitrary vector beams with tunable polarization, phase, and amplitude," *Photonics Res.* **6**, 228–233 (2018).
- ²⁰⁶P. Li, Y. Zhang, S. Liu, H. Cheng, L. Han, D. Wu, and J. Zhao, "Generation and self-healing of vector Bessel-Gauss beams with variant state of polarizations upon propagation," *Opt. Express* **25**, 5821–5831 (2017).
- ²⁰⁷A. Aleksanyan and E. Brasselet, "Spin-orbit photonic interaction engineering of Bessel beams," *Optica* **3**, 167–174 (2016).
- ²⁰⁸S. Vyas, Y. Kozawa, and Y. Miyamoto, "Creation of polarization gradients from superposition of counter propagating vector LG beams," *Opt. Express* **23**, 33970–33979 (2015).
- ²⁰⁹H. Li, V. Rodrigues-Fajardo, P. Chen, and A. Forbes, "Angular momentum conservation in counter-propagating vectorially structured light," *arXiv:2005.02739* (2020).
- ²¹⁰K. Y. Bliokh, M. A. Alonso, E. A. Ostrovskaya, and A. Aiello, "Angular momenta and spin-orbit interaction of nonparaxial light in free space," *Phys. Rev. A* **82**, 063825 (2010).
- ²¹¹S. M. Barnett and L. Allen, "Orbital angular momentum and nonparaxial light beams," *Opt. Commun.* **110**, 670–678 (1994).
- ²¹²T. A. Nieminen, A. B. Stilgoe, N. R. Heckenberg, and H. Rubinsztein-Dunlop, "Angular momentum of a strongly focused Gaussian beam," *J. Opt. A: Pure Appl. Opt.* **10**, 115005 (2008).
- ²¹³A. Y. Bekshaev, "A simple analytical model of the angular momentum transformation in strongly focused light beams," *Cent. Eur. J. Phys.* **8**, 947–960 (2010).
- ²¹⁴Z. Bomzon, M. Gu, and J. Shamir, "Angular momentum and geometrical phases in tight-focused circularly polarized plane waves," *Appl. Phys. Lett.* **89**, 241104 (2006).
- ²¹⁵Y. Zhao, J. S. Edgar, G. D. Jeffries, D. McGloin, and D. T. Chiu, "Spin-to-orbital angular momentum conversion in a strongly focused optical beam," *Phys. Rev. Lett.* **99**, 073901 (2007).
- ²¹⁶A. V. Arzola, L. Chvátal, P. Ják, and P. Zemánek, "Spin to orbital light momentum conversion visualized by particle trajectory," *Sci. Rep.* **9**, 4127 (2019).
- ²¹⁷M. Michihata, T. Hayashi, and Y. Takaya, "Measurement of axial and transverse trapping stiffness of optical tweezers in air using a radially polarized beam," *Appl. Opt.* **48**, 6143–6151 (2009).
- ²¹⁸M.-C. Zhong, L. Gong, D. Li, J.-H. Zhou, Z.-Q. Wang, and Y.-M. Li, "Optical trapping of core-shell magnetic microparticles by cylindrical vector beams," *Appl. Phys. Lett.* **105**, 181112 (2014).
- ²¹⁹M. Donato, S. Vasi, R. Sayed, P. Jones, F. Bonaccorso, A. Ferrari, P. Gucciardi, and O. Maragò, "Optical trapping of nanotubes with cylindrical vector beams," *Opt. Lett.* **37**, 3381–3383 (2012).
- ²²⁰H. Moradi, V. Shahabadi, E. Madadi, E. Karimi, and F. Hajizadeh, "Efficient optical trapping with cylindrical vector beams," *Opt. Express* **27**, 7266–7276 (2019).
- ²²¹M. Li, S. Yan, Y. Zhang, Y. Liang, P. Zhang, and B. Yao, "Optical sorting of small chiral particles by tightly focused vector beams," *Phys. Rev. A* **99**, 033825 (2019).
- ²²²G. Milione, H. I. Sztul, D. A. Nolan, and R. R. Alfano, "Higher-order Poincaré sphere, Stokes parameters, and the angular momentum of light," *Phys. Rev. Lett.* **107**, 053601 (2011).

- ²²³E. Otte, K. Tekce, S. Lamping, B. J. Ravoo, and C. Denz, "Polarization nanotomography of tightly focused light landscapes by self-assembled monolayers," *Nat. Commun.* **10**, 4308 (2019).
- ²²⁴N. Bokor and N. Davidson, "Generation of a hollow dark spherical spot by 4pi focusing of a radially polarized Laguerre-Gaussian beam," *Opt. Lett.* **31**, 149–151 (2006).
- ²²⁵H. Wang, L. Shi, B. Lukyanchuk, C. Sheppard, and C. T. Chong, "Creation of a needle of longitudinally polarized light in vacuum using binary optics," *Nat. Photonics* **2**, 501–505 (2008).
- ²²⁶F. Qin, K. Huang, J. Wu, J. Jiao, X. Luo, C. Qiu, and M. Hong, "Shaping a sub-wavelength needle with ultra-long focal length by focusing azimuthally polarized light," *Sci. Rep.* **5**, 9977 (2015).
- ²²⁷Y. Zhao, Q. Zhan, Y. Zhang, and Y.-P. Li, "Creation of a three-dimensional optical chain for controllable particle delivery," *Opt. Lett.* **30**, 848–850 (2005).
- ²²⁸Z. Man, Z. Bai, S. Zhang, X. Li, J. Li, X. Ge, Y. Zhang, and S. Fu, "Redistributing the energy flow of a tightly focused radially polarized optical field by designing phase masks," *Opt. Express* **26**, 23935–23944 (2018).
- ²²⁹M. Li, S. Yan, Y. Zhang, P. Zhang, and B. Yao, "Enantioselective optical trapping of chiral nanoparticles by tightly focused vector beams," *J. Opt. Soc. Am. B* **36**, 2099–2105 (2019).
- ²³⁰E. J. Galvez, I. Dutta, K. Beach, J. J. Zeosky, J. A. Jones, and B. Khajavi, "Multitwist Möbius strips and twisted ribbons in the polarization of paraxial light beams," *Sci. Rep.* **7**, 13653 (2017).
- ²³¹C. Wan and Q. Zhan, "Generation of exotic optical polarization Möbius strips," *Opt. Express* **27**, 11516–11524 (2019).
- ²³²A. Garcia-Etxarri, "Optical polarization Möbius strips on all-dielectric optical scatterers," *ACS Photonics* **4**, 1159–1164 (2017).
- ²³³T. Bauer, P. Banzer, F. Bouchard, S. Orlov, L. Marrucci, E. Santamato, R. W. Boyd, E. Karimi, and G. Leuchs, "Multi-twist polarization ribbon topologies in highly-confined optical fields," *New J. Phys.* **21**, 053020 (2019).
- ²³⁴P. Huo, S. Zhang, Q. Fan, Y. Lu, and T. Xu, "Photonic spin-controlled generation and transformation of 3D optical polarization topologies enabled by all-dielectric metasurfaces," *Nanoscale* **11**, 10646–10654 (2019).
- ²³⁵T. Bauer, M. Neugebauer, G. Leuchs, and P. Banzer, "Optical polarization Möbius strips and points of purely transverse spin density," *Phys. Rev. Lett.* **117**, 013601 (2016).
- ²³⁶L. Novotny, M. R. Beversluis, K. S. Youngworth, and T. G. Brown, "Longitudinal field modes probed by single molecules," *Phys. Rev. Lett.* **86**, 5251–5254 (2001).
- ²³⁷N. Rotenberg and L. Kuipers, "Mapping nanoscale light fields," *Nat. Photonics* **8**, 919 (2014).
- ²³⁸T. Bauer, S. Orlov, U. Peschel, P. Banzer, and G. Leuchs, "Nanointerferometric amplitude and phase reconstruction of tightly focused vector beams," *Nat. Photonics* **8**, 23–27 (2014).
- ²³⁹A. Marzo and B. W. Drinkwater, "Holographic acoustic tweezers," *Proc. Natl. Acad. Sci. U. S. A.* **116**, 84–89 (2019).
- ²⁴⁰K. Y. Bliokh and F. Nori, "Spin and orbital angular momenta of acoustic beams," *Phys. Rev. B* **99**, 174310 (2019).
- ²⁴¹E. Toninelli, M. A. Cox, G. M. Gibson, S. D. Brown, M. P. Edgar, A. Forbes, and M. J. Padgett, "A compact acoustic spanner to rotate macroscopic objects," *Sci. Rep.* **9**, 6757 (2019).
- ²⁴²F. Nan and Z. Yan, "Silver-nanowire-based interferometric optical tweezers for enhanced optical trapping and binding of nanoparticles," *Adv. Funct. Mater.* **29**, 1808258 (2019).
- ²⁴³J. Berthelot, S. Aćimović, M. Juan, M. Kreuzer, J. Renger, and R. Quidant, "Three-dimensional manipulation with scanning near-field optical nanotweezers," *Nat. Nanotechnol.* **9**, 295–299 (2014).
- ²⁴⁴Y. Pang and R. Gordon, "Optical trapping of a single protein," *Nano Lett.* **12**, 402–406 (2012).
- ²⁴⁵C. Min, Z. Shen, J. Shen, Y. Zhang, H. Fang, G. Yuan, L. Du, S. Zhu, T. Lei, and X. Yuan, "Focused plasmonic trapping of metallic particles," *Nat. Commun.* **4**, 2891 (2013).
- ²⁴⁶A. Selyem, S. Fayard, T. W. Clark, A. S. Arnold, N. Radwell, and S. Franke-Arnold, "Holographically controlled three-dimensional atomic population patterns," *Opt. Express* **26**, 18513–18522 (2018).
- ²⁴⁷G. Gauthier, I. Lenton, N. M. Parry, M. Baker, M. J. Davis, H. Rubinsztein-Dunlop, and T. W. Neely, "Direct imaging of a digital-micromirror device for configurable microscopic optical potentials," *Optica* **3**, 1136–1143 (2016).